THE JOURNAL OF COMPARATIVE NEUROLOGY 400:207–228 (1998)

Noradrenergic System of the Zebra Finch Brain: Immunocytochemical Study of Dopamine-β-Hydroxylase

CLAUDIO V. MELLO,[1]* RAPHAEL PINAUD,[1,2] AND SIDARTA RIBEIRO[1]
[1]Laboratory of Animal Behavior, The Rockefeller University, New York, New York 10021
[2]Laboratório de Neurobiologia II, Instituto de Biofísica, Federal University of Rio de Janeiro (UFRJ), 21941–900 Brazil

ABSTRACT

Oscine birds are among the few animal groups that have vocal learning, and their brains contain a specialized system for song learning and production. We describe here the immunocytochemical distribution of dopamine-β-hydroxylase (DBH), a noradrenergic marker, in the brain of an oscine, the zebra finch (*Taeniopygia guttata*). DBH-positive cells were seen in the locus coeruleus, the nucleus subcoeruleus ventralis, the nucleus of the solitary tract, and the caudolateral medulla. Immunoreactive fibers and varicosities had a much wider brain distribution. They were particularly abundant in the hippocampus, septum, hypothalamus, area ventralis of Tsai, and substantia nigra, where they formed dense pericellular arrangements. Significant immunoreactivity was observed in auditory nuclei, including the nucleus mesencephalicus lateralis pars dorsalis, the thalamic nucleus ovoidalis, field L, the shelf of the high vocal center (HVC), and the cup of the nucleus robustus archistriatalis (RA), as well as in song control nuclei, including the HVC, RA, the lateral magnocellular nucleus of the anterior neostriatum, and the dorsomedial nucleus (DM) of the intercollicular complex. Except for the DM, DBH immunoreactivity within song nuclei was comparable to that of surrounding tissues. Conspicuously negative were the lobus paraolfactorius, including song nucleus area X, and the paleostriatum. Our results are in agreement with previous studies of the noradrenergic system performed in nonoscines. More importantly, they provide direct evidence for a noradrenergic innervation of auditory and song control nuclei involved in song perception and production, supporting the notion that noradrenaline is involved in vocal communication and learning in oscines. J. Comp. Neurol. 400:207–228, 1998.

Indexing terms: catecholamines; norepinephrine; avian; songbirds; song system; HVC

Song learning in oscines occurs through imitation of an auditory model (Thorpe, 1958; Marler and Tamura, 1964; Konishi, 1965; Nottebohm, 1968, 1972; Marler and Peters, 1977, 1981, 1982; Kroodsma, 1982) and depends on a set of discrete, interconnected brain nuclei (Nottebohm et al., 1976; Bottjer et al., 1984; Sohrabji et al., 1990; Scharff and Nottebohm, 1991). These are known collectively as the song system, and they ultimately control the function of the vocal organ, the syrinx. The connectivity of song control nuclei has been characterized in detail (Nottebohm et al., 1982; Okuhata and Saito, 1987; Bottjer et al., 1989; Vicario and Nottebohm, 1990; Vicario, 1991, 1993; Wild, 1993, 1994; Johnson et al., 1995; Vates and Nottebohm, 1995; for a recent review, see Wild, 1997). Briefly, the high vocal center (HVC), a site of sensorimotor integration, projects onto the robust nucleus of the archistriatum (RA). RA, in turn, projects directly to motoneurons of the XII cranial nerve that innervate the syrinx; RA also projects indirectly to these motoneurons through the dorsomedial nucleus (DM) of the intercollicular complex (ICo). HVC and RA fire in conjunction with singing behavior (Yu and Margoliash, 1996), and their integrity is essential for normal song production (Nottebohm et al., 1976). These nuclei are underdeveloped or absent in females, which often sing little or not at all (for instance, see review by Arnold, 1997). HVC also projects indirectly to RA through a distinct pathway that includes area X of the paleostriatum, the medial nucleus of the dorsolateral thalamus (DLM), and the lateral magnocellular nucleus of the

Grant sponsor: NIDCD; Grant number: DC02853.

*Correspondence to: Claudio V. Mello, M.D., Ph.D., Laboratory of Animal Behavior, The Rockefeller University, 1230 York Avenue, New York, NY 10021. E-mail: mello@rockvax.rockefeller.edu

Received 23 February 1998; Revised 5 June 1998; Accepted 17 June 1998

anterior neostriatum (lMAN). This rostral pathway is essential for song learning in juveniles and apparently is not necessary for normal song production in adults (Bottjer et al., 1984; Sohrabji et al., 1990; Scharff and Nottebohm, 1991), although recent evidence from gene expression studies indicates its activation during active singing (Jarvis and Nottebohm, 1997; Mello and Ribeiro, 1998). Finally, considerable effort has also been devoted to describing the central auditory pathways in songbirds (Kelley and Nottebohm, 1979; Fortune and Margoliash, 1992, 1995; Vates et al., 1996; Mello et al., 1998); these pathways presumably play an important role in the processing and storage of song auditory information as well as in the auditory-vocal integration upon which vocal learning depends.

Catecholamines, in particular noradrenaline, have been implicated in synaptic plasticity and neural control of learning in several systems (Everitt et al., 1983; Hopkins and Johnston, 1984; McGaugh, 1989; Sullivan et al., 1989; Wilson et al., 1994). The possibility that catecholamines are also involved in bird song learning and production has been supported by evidence from a variety of experimental approaches. These include measurement of catecholamine levels and turn-over rates as well as the detection of their receptors in song control nuclei (Lewis et al., 1981; Sakaguchi and Saito, 1989; Ball, 1990, 1994; Ball et al., 1994; Casto and Ball, 1996; Harding et al., 1998), the demonstration of their modulation within song nuclei by sex steroids (Barclay and Harding, 1988, 1990), and immunocytochemical (ICC) studies of the brain distribution of tyrosine

Abbreviations

A	archistriatum
An	nucleus angularis
ANI	nucleus annularis
AP	area pretectalis
AVT	area ventralis (Tsai)
Cb	cerebellum
CbN	cerebellar nuclei
cHV	caudal hyperstriatum ventrale
CO	optic chiasm
CoA	anterior commissure
CoS	nucleus commissuralis septi
CP	posterior commissure
DBC	decussatio brachiorum conjunctivorum
DIP	nucleus dorsointermedius posterior thalami
DLA	nucleus dorsolateralis anterior thalami, pars magnocellularis
DLM	nucleus dorsolateralis anterior thalami, pars medialis
DLP	nucleus dorsolateralis posterior thalami
DM	dorsomedial nucleus of the ICo
DMP	posterior nucleus of the dorsomedial thalamus
DSD	decussatio supraoptica dorsalis
E	ectostriatum
FA	tractus frontoarchistriatalis
FLM	fasciculus longitudinalis medialis
FPL	fasciculus prosencephali lateralis (lateral forebrain bundle)
GCT	substantia grisea centralis
GLV	nucleus geniculatus lateralis, pars ventralis
H	hyperstriatum
HA	hyperstriatum accessorium
Hb	nucleus habenularis
Hp	hippocampus
HV	hyperstriatum ventrale
HVC	high vocal center
Hy	hypothalamus
ICo	nucleus intercollicularis
ICT	nucleus intercalatus thalami
IM	nucleus isthmi, pars magnocellularis
IO	nucleus isthmoopticus
IP	nucleus interpeduncularis
IPC	nucleus isthmi, pars parvocellularis
L1, L2a, L3	field L subdivisions
LA	nucleus lateralis anterior thalami
La	nucleus laminaris
LHy	nucleus lateralis hypothalami
lMAN	lateral magnocellular nucleus of the anterior neostriatum
LoC	locus coeruleus
LPO	lobus paraolfactorius
MC	nucleus magnocellularis
MLd	nucleus mesencephalicus lateralis, pars dorsalis
MPv	nucleus mesencephalicus profundus ventralis
N	neostriatum
NC	caudal neostriatum
NCM	caudomedial neostriatum
NIf	nucleus interfascialis
NIII	oculomotor nerve
NIV	trochlear nerve
nIV	nucleus of the trochlear nerve
nIX–nX	nucleus of the glossopharyngeal nerve and dorsal motor nucleus of the vagal nerve
nVI	nucleus of the abducens nerve
NVIII	octaval nerve
nXII	nucleus of the hypoglossal nerve
OI	inferior olive
OM	tractus occipitomesencephalicus
OMd	nucleus nervi oculomotorii, pars dorsalis
OMv	nucleus nervi oculomotorii, pars ventralis
OS	superior olivary nucleus
Ov	nucleus ovoidalis
P	paleostriatum
PA	paleostriatum augmentatum
Pc	caudodorsal paleostriatum
PM	nucleus pontis medialis
PMI	nucleus paramedianus internis thalami
POM	nucleus preopticus medialis
PP	paleostriatum primitivum
PrV	nucleus sensorius principalis nervi trigemini
Pt	nucleus pretectalis
PV	nucleus posteroventralis thalami
PVN	nucleus paraventricularis magnocellularis
R	reticular formation
RA	robust nucleus of the archistriatum
Rt	nucleus rotundus
Ru	nucleus ruber
S	nucleus of the solitary tract
SAC	stratum album centrale
SCE	stratum cellulare externum
SCI	stratum cellulare internum
SCv	nucleus subcoeruleus ventralis
Se	septum
SGC	stratum griseum centrale
SGF	stratum griseum et fibrosum superficiale
Sh	shelf
SLu	nucleus semilunaris
SM	nucleus septalis medialis
SN	substantia nigra
SOp	stratum opticum
SpL	nucleus spiriformis lateralis
SpM	nucleus spiriformis medialis
Ta	nucleus tangentialis
TeO	optic tectum
ToS	torus semicircularis
tOv	tractus ovoidalis
TPc	nucleus tegmenti pedunculopontinus, pars compacta
TrO	optic tract
TrSM	tractus septomesencephalicus
TTD	nucleus et tractus descendens nervi trigemini
Tu	nucleus tuberis
TV	nucleus tegmenti ventralis
Uva	nucleus uvaeformis
V	ventricle
VeL	nucleus vestibularis lateralis
VeM	nucleus vestibularis medialis
VLT	nucleus ventrolateralis thalami
VLV	ventral nucleus of the lateral lemniscus
VMN	nucleus ventromedialis hypothalami
VS	nucleus vestibularis superior
X	area X of the paraolfactory lobe

hydroxylase (TH; Bottjer, 1993; Soha et al., 1996). The latter revealed a rich innervation of several telencephalic song nuclei, including HVC, RA, and area X. This innervation develops between 30 and 60 days posthatch, which is well within the sensitive period for song acquisition in juveniles (Immelman, 1969; Eales, 1985, 1987), persisting into adulthood.

TH, however, is present in all cells that are known to synthesize catecholamines, because it is the rate-limiting enzyme in this biosynthetic pathway. Therefore, it does not differentiate among the different classes of catecholaminergic cells. In contrast, dopamine-β-hydroxylase (DBH) catalyzes the conversion of dopamine to noradrenaline and is thought not to be present at significant levels in dopaminergic cells; thus, it constitutes a more selective marker than TH for noradrenergic cells. DBH brain immunoreactivity has been described previously in nonoscines, including the quail (Bailhache and Balthazart, 1993), the pigeon (Reiner et al., 1994), and the chicken (Moons et al., 1995). These avian species, however, do not possess a developed song control system and are not known to depend on auditory feedback to develop their species-specific vocalizations. ICC studies using specific noradrenergic markers in oscines, which possess a specialized brain system for vocal learning and production, are still lacking. This is an important gap in our current understanding of the organization of the noradrenergic system in the avian brain.

We describe here the brain distribution of DBH immunoreactivity (DBH-ir) in an oscine species, the zebra finch (*Taeniopygia guttata*), in which the auditory and song control systems have been characterized in particular detail. We have focused our analysis on brain areas that are thought to play some role in the processes of song learning, perception, or production. The general distribution of DBH-ir that we observed was in close agreement with previous descriptions of the avian noradrenergic system. A differential comparison of DBH-ir distribution with the known TH-staining pattern in the zebra finch (Bottjer, 1993) allows significant inferences to be drawn about the organization of the dopaminergic system. We also demonstrate a marked noradrenergic innervation of several auditory stations and song control nuclei, providing support for a role of noradrenaline in the neurobiology of bird song.

MATERIALS AND METHODS

Animals

A total of 18 zebra finches were studied, consisting of eight adults (six males and two females) and ten juveniles (two each at 25, 35, 39, 45, and 60 days of age). The birds were bred in indoor aviaries at the Rockefeller University's Field Research Center in Millbrook, New York. Handling and killing of animals was approved by the Rockefeller University's Laboratory Animal Research Center and was carried out according to National Institutes of Health guidelines.

ICC

Birds were killed under deep Nembutal anesthesia and were perfused sequentially with phosphate-buffered saline (PBS), pH 7.4, and 4% paraformaldehyde in 0.1 M phosphate buffer (PB), pH 7.4. Brains were then dissected out, washed overnight at 4°C in 0.1 M PB under agitation, sunken in 20% sucrose in 0.1 M PB, and frozen in embedding medium (TissueTek; Sakura Finetek, Torrance, CA) in a dry-ice/ethanol bath. Twenty-micrometer sections were cut on a cryostat, mounted onto slides that were precoated with chromalum or 3-aminopropyl triethoxysilane (TESPA; Aldrich, Milwaukee, WI), and air dried overnight. The sections were cut in the frontal plane ($n = 3$ adult males) or in the parasagittal plane, starting from the midline (all other animals). Slides were then incubated sequentially as follows: 1) 30 minutes at room temperature in blocking solution (0.5% skim milk and 0.3% Triton X-100 in 0.1 M PB), 2) 36–48 hours at 4°C in blocking solution containing a rabbit anti-bovine-DBH antiserum (1:1,000; Eugene Tech, Ridgefield Park, NJ), 3) 15 minutes at room temperature in avidin blocking solution followed by 15 minutes at room temperature in biotin blocking solution at the dilution recommended by the manufacturer (Vector blocking kit; Vector Laboratories, Burlingame, CA), 4) 2 hours at room temperature in blocking solution containing biotinylated goat anti-rabbit immunoglobulin G (IgG; 1:200, Vector Laboratories), and 5) 2 hours at room temperature in avidin-biotin complex (ABC) reagent at the dilution recommended by the manufacturer (Vector Laboratories). Each of the steps above was followed by three washes (10 minutes each) in 0.1 M PB, pH 7.4. The slides were then developed by incubation in 0.03% diaminobenzidine (DAB), 0.15% nickel-ammonium sulfate, and 0.001% H_2O_2 in PB followed by rinsing in PB, dehydration, and coverslipping with Permount. To assess the specificity of our detection system, ICC controls were run as described above but omitting incubations with either the primary or secondary antisera.

Adjacent sections were stained with cresyl violet to allow visualization of brain structures. The identification and anatomical nomenclature of telencephalic, diencephalic, and mesencephalic areas were based on the canary atlas (Stokes et al., 1974), with some adjustments, as well as on previous anatomical studies of the organization of the song control system (listed above) and auditory processing areas in zebra finches (Fortune and Margoliash, 1992; Vates et al., 1996). The identification of hypothalamic nuclei (such as the nucleus preopticus medialis [POM] and the nucleus paraventricularis magnocellularis [PVN]; Figs. 2, 9) was based on previous neurochemical mapping studies (Balthazart et al., 1996). For analysis of caudal pontine and medullary regions, we relied primarily on the pigeon (Karten and Hodos, 1967) and chicken (Kuenzel and Mason, 1988) atlases, because the canary atlas does not include structures caudal to the rostral pons. It remains to be determined, however, whether there is a strict correspondence between caudal brainstem structures of nonoscines and oscines. Our results were also compared closely with previous reports of TH- and DBH-staining patterns in oscines and nonoscines (Bailhache and Balthazart, 1993; Bottjer, 1993; Reiner et al., 1994; Moons et al., 1995).

Data analysis

Two sets of serial sections (one parasagittal and one frontal) were stained with cresyl violet and drawn under the microscope with a camera lucida (10× objective). These drawings served as a set of reference sections onto which a general brain map of DBH-ir was represented. For that purpose, we examined in detail the staining patterns of all brains under the microscope and generated a classification scheme based on the relative density of immunoreactive elements. Four different categories or staining

patterns were readily apparent, and they typify the patterns encountered in our analysis (for details, see Results), as shown by the photomicrographic images in Figure 1. The various brain regions and nuclei that were analyzed were assigned to one of the categories described above (by comparison with these images) to generate the maps presented in Figures 2 and 3. Pictures of various brain areas and nuclei were also taken to document morphological details of the immunoreactive elements observed. Comparisons with DBH staining patterns in females and juveniles were performed blind by direct inspection under the microscope.

Figure preparation

For Figures 2 and 3, camera lucida drawings were made on an Olympus microscope (Tokyo, Japan), scanned in a flat-bed scanner (Color One scanner; Apple Computers, Cupertino, CA), and composed by using Freehand software (Macromedia, San Francisco, CA). For all other figures, selected fields in stained sections were digitized directly by using a black-and-white CCD camera (300 dpi; Hitachi, Saitama, Japan) coupled to a microscope (model IX70; Olympus), and image-processing software (NIH Image, Bethesda, MD). For each photomicrograph, several adjacent images covering the area of interest were captured at high magnification by using 20× or 40× objectives (Olympus). Photoshop software (Adobe Systems, Mountain View, CA) was then used to assemble the partial images into final composite images, to adjust gray levels, and for figure formatting and lettering without any modifications to the data.

RESULTS

We observed a widespread distribution of DBH-ir in the brain of adult male zebra finches, as described previously for other avian species and mammals. Labeled fibers and varicosities could be seen throughout most brain regions, their local density varying markedly across different areas. Labeled cell bodies, in contrast, were present only in the caudal brainstem and lower structures. This general pattern is represented in Figures 1–3 and is described below in detail for each brain subdivision. Unless stated otherwise, we used the series of frontal sections (Fig. 2) to describe the staining patterns of the septum, diencephalon, brainstem, and lower structures and the series of parasagittal sections (Fig. 3) for telencephalic structures. After an extensive blind analysis of all animals studied, no obvious age or sex differences in the DBH staining patterns were observed. None of the DBH-ir elements described below were seen in the ICC controls.

DBH-labeled cells

DBH-labeled perikarya had a very restricted distribution, being confined to the caudal midbrain, pons, and caudal portion of the medulla. Following the rostrocaudal axis, the first group of labeled cells was seen in the ventrolateral portion of the caudal end of the mesencephalon (Fig. 2G,H), starting at a level slightly caudoventral to the posterior end of the avian substantia nigra (SN), formerly named the nucleus tegmenti pedunculopontinus pars compacta, or TPc (Fig. 2F). The distribution of this cell group corresponded largely to, but extended beyond, the Nissl-defined boundaries of the area identified as the nucleus subcoeruleus ventralis (SCv). The area occupied by these cells was elongated in the ventrolateral to dorsomedial direction, and cell bodies typically were oriented along this axis (Figs. 2G, 4A). The cells were characterized by rather large, typically triangular cell bodies with numerous dendritic processes and extensive arborizations (Fig. 4E). At the level of the nucleus and emergence of the trochlearis nerve (nIV; NIV), the cells became smaller and were displaced dorsomedially (Figs. 2H, 4B). Farther caudally, this cell group became more diffuse, and, finally, it was substituted by a dense bed of fibers and varicosities (not shown). Some scattered, labeled cells extended rostrally as far as the region immediately ventral to the SN (Fig. 2F). Because it was difficult to assess the exact caudal boundary of the SN based on cytoarchitectonic features in Nissl-stained material alone, there is a small possibility that a few of these cells were actually within the very caudal portion of this nucleus.

A second, distinct group of DBH-positive cells was located in the dorsorostral pons and pontine-mesencephalic transition immediately caudal to the nIV. This location corresponded to the locus coeruleus (LoC; Fig. 2I). The cells here were smaller than cells in the SCv and, typically, had round- or oval-shaped perikarya, strongly stained cytoplasm, and conspicuously unstained nuclei (Fig. 4F). The relationship between the spatial distribution of labeled cells in the LoC and the SCv can be appreciated best as one moves along the mediolateral axis in the series of parasagittal sections (Figs. 3B,C, 4C,D). A few scattered cell bodies were also observed immediately caudal to the LoC in the vicinity of the nucleus vestibularis medialis (VeM; not shown). Some scattered, labeled cell bodies could also be seen in the ventrolateral portion of the caudal pons in loose association with nuclei of the reticular formation and superior olive (Fig. 2I,J).

Farther caudally, in the medulla, three other distinct groups of labeled cells were seen. The first group consisted of a few scattered multipolar cells located in the ventrolateral portion of the rostral medulla in loose association with nuclei of the reticular formation (not shown). The second group was located dorsomedially, surrounding the nucleus of the solitary tract (S) and the nuclei of the glossopharyngeal and vagal nerves (nIX–X; Figs. 2M,N, 4G). These were small cells, and the labeling was weaker than that seen in the LoC. Most cells appeared to occur outside S and dorsolateral to nIX–X, although a few labeled cells could be seen occasionally within S as well (not shown). The third group consisted of small numbers of strongly labeled cells that were scattered throughout the lateral portion of the caudal medulla, possibly extending into the first cervical segment (Figs. 2N, 4H).

DBH-labeled fibers

DBH immunostaining varied significantly throughout the brain, ranging locally from sites where immunoreactive elements were scarce or absent to sites with a high abundance of labeled fibers and varicosities. We classified the staining patterns into four general categories, depending on whether DBH-ir was absent or scarce (1); present in moderate amounts (2); fairly abundant (3); and highly dense, often forming intricate pericellular arrays (4). Figure 1 shows representative images of these four groups, which consist, respectively, of the paleostriatum (Fig. 1A), the caudomedial neostriatum (Fig. 1B), the rostral neostriatum (Fig. 1C), and the hippocampus (Fig. 1D). This classification scheme provides a key to the density of labeled fibers

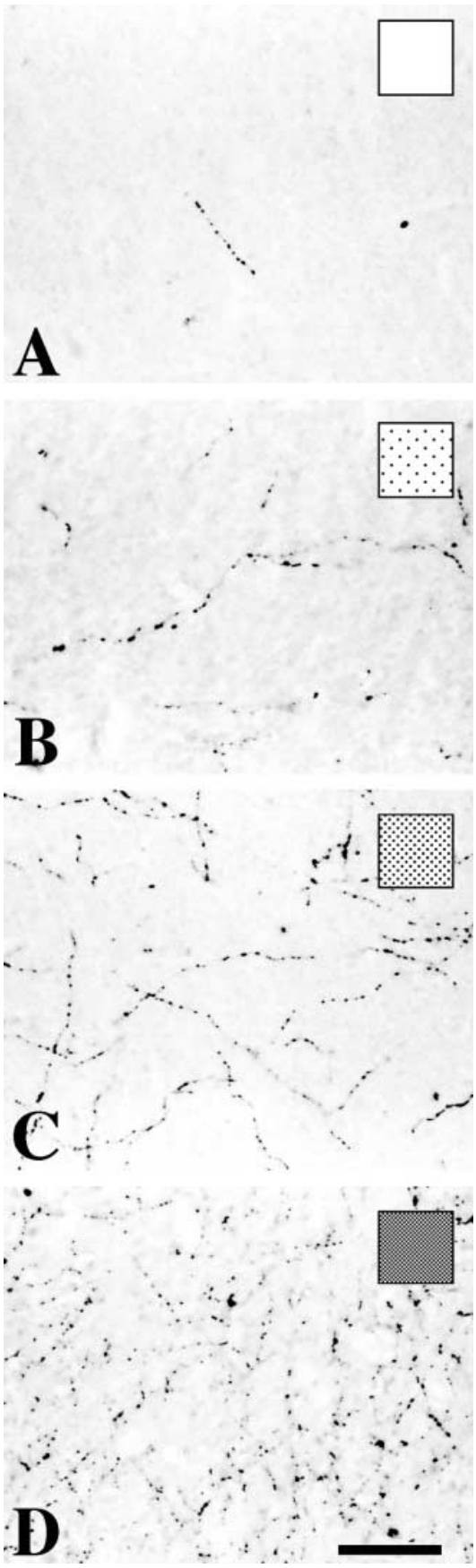

shown in the maps in Figures 2 and 3. The general maps of DBH-ir as well as salient morphological features are described below for each major brain subdivision.

In several brain regions, two kinds of dense pericellular arrangements could be seen. One consisted of abundant DBH-positive elements in the neuropil surrounding negative perikarya and dendrites, resulting in a dense array of staining that resembled a honeycomb (for example, see Fig. 9B,D). The other consisted of numerous punctate, DBH-positive elements covering the surface of DBH-negative cell somata and dendritic processes (for examples, see Figs. 11C, 13C, 14A); the density of these elements was such that the cells tended to be confused at low power with immunopositive cell bodies.

Telencephalon. In general, DBH-ir elements in the telencephalon tended to be oriented in a rostrocaudal direction. Thus, the series of parasagittal sections (Fig. 3) was particularly suitable for analyzing in detail the telencephalic distribution of DBH. The highest density of immunoreactive fibers and varicosities was seen in the hippocampus (Hp), particularly in its most medial portions (Fig. 3A). The fibers ascended vertically from the septal region, running in parallel to form a palisade in the ventromedial Hp (Fig. 5A). More dorsally, these elements assumed a more reticular aspect (for detail, see Fig. 1D), with some large immunonegative perikarya surrounded by a dense net of fine branches and varicosities (not shown).

The overall density of immunoreactive elements then decreased as one progressed laterally. The rostromedial portion of the neostriatum, hyperstriatum ventrale, hyperstriatum accessorium, and archistriatum had fairly high densities of immunoreactivity (Fig. 3B,C). Within the rostral neostriatum, the fibers clearly were disposed along the rostrocaudal axis (Fig. 5B), whereas, in

Fig. 1. High-power images depicting distinct patterns of dopamine-β-hydroxylase (DBH)-immunoreactive staining in different regions of the zebra finch brain. The areas shown are the paleostriatum augmentatum (**A**), the caudomedial neostriatum (**B**), the rostromedial neostriatum (**C**), and the hippocampus (**D**). The general brain distribution of these patterns is shown in Figures 2 and 3. **Insets** in the upper right corners in A–D (black dots) provide keys to the density maps in those figures. Scale bar = 50 μm.

Fig. 2. (overleaf) **A–N:** Maps of the distribution of DBH immunoreactivity (DBH-ir; black dots) in the zebra finch basal forebrain, diencephalon, brainstem, and lower structures. The distinct patterns of DBH-ir (for keys, see Fig. 1) were mapped onto camera lucida drawings of a series of frontal sections. Except for the ventromedial portion of the paleostriatum (A–D), telencephalic structures are not represented. Brain areas in which the boundaries are distinctly recognizable in sections stained with cresyl violet are encircled by solid lines; the boundaries of the medial preoptic nucleus (POM) are represented by the dashed line in A–C (in accordance with Balthazart et al., 1996). Solid triangles indicate the location where labeled somata occur, and open triangles represent the location of dense arrangements of DBH-positive elements surrounding negative perikarya. A–I correspond respectively to the planes A2.6, A2.2, A1.6, A0.8, A0.4, A0.2, P0.6, P1.2, and P1.6 of the canary atlas (Stokes et al., 1974); J–N correspond approximately to the planes AP0.00, P0.5, P1.25, P3.00, and P3.75 of the pigeon atlas (Karten and Hodos, 1967). The area at the transition between the ventromedial paraolfactory lobe (LPO) and the dorsal hypothalamus indicated by an asterisk in A–C is shown in detail in Figure 8A. Orientation: For this and all other figures that were derived from frontal sections, dorsal is up. For abbreviations, see list. Scale bar = 1 mm.

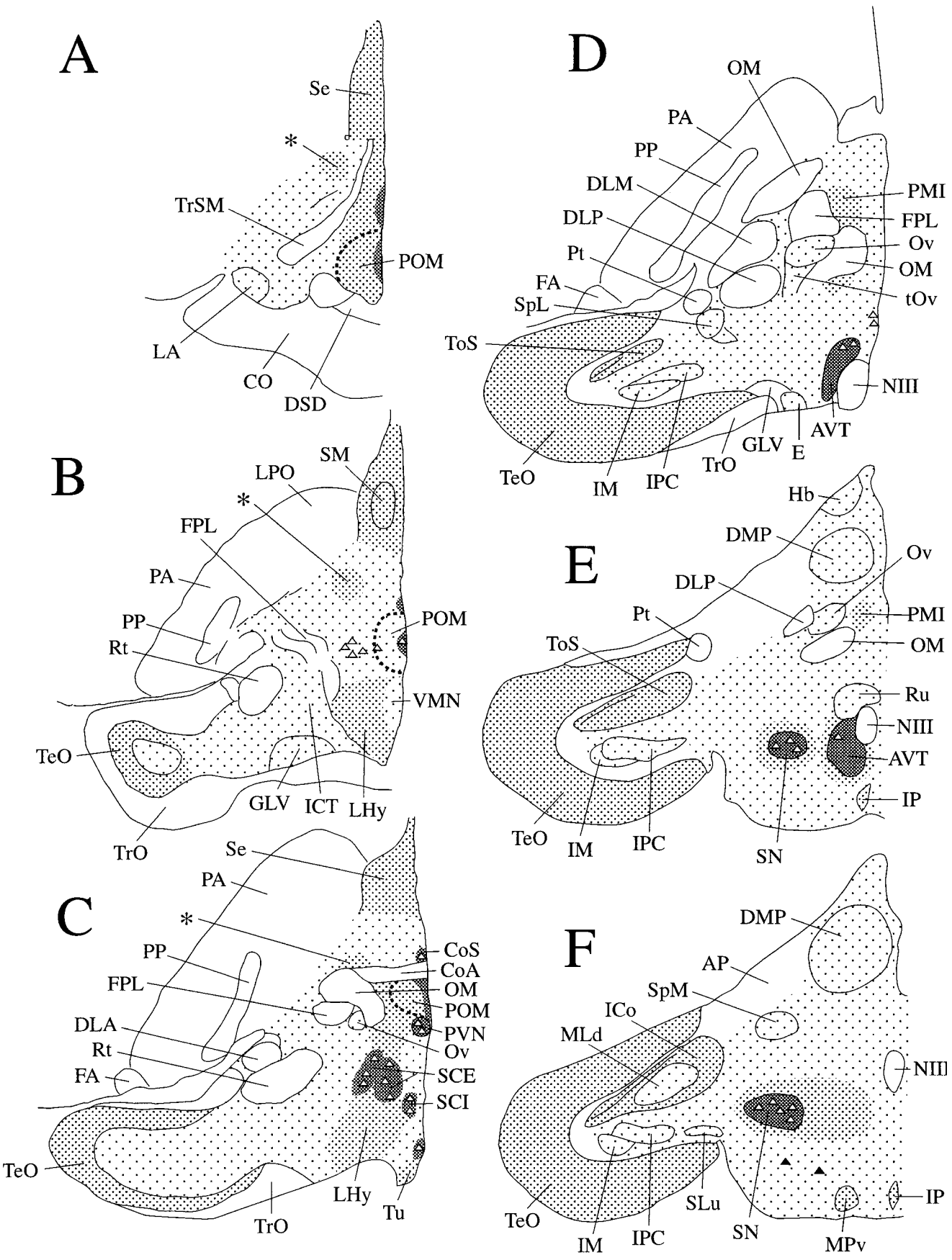
A
Se
*
TrSM
POM
LA
CO
DSD
B
SM
LPO
*
FPL
PA
PP
Rt
POM
VMN
TeO
GLV
ICT
LHy
TrO
C
Se
PA
*
PP
FPL
DLA
Rt
FA
CoS
CoA
OM
POM
PVN
Ov
SCE
SCI
TeO
LHy
Tu
TrO
D
OM
PA
PP
DLM
DLP
Pt
FA
SpL
ToS
PMI
FPL
Ov
OM
tOv
NIII
AVT
GLV
E
TrO
TeO
IM
IPC
E
Hb
DMP
Ov
DLP
Pt
ToS
PMI
OM
Ru
NIII
AVT
IP
TeO
IM
IPC
SN
F
DMP
AP
SpM
ICo
MLd
NIII
IP
SLu
TeO
IM
IPC
SN
MPv

Figure 2

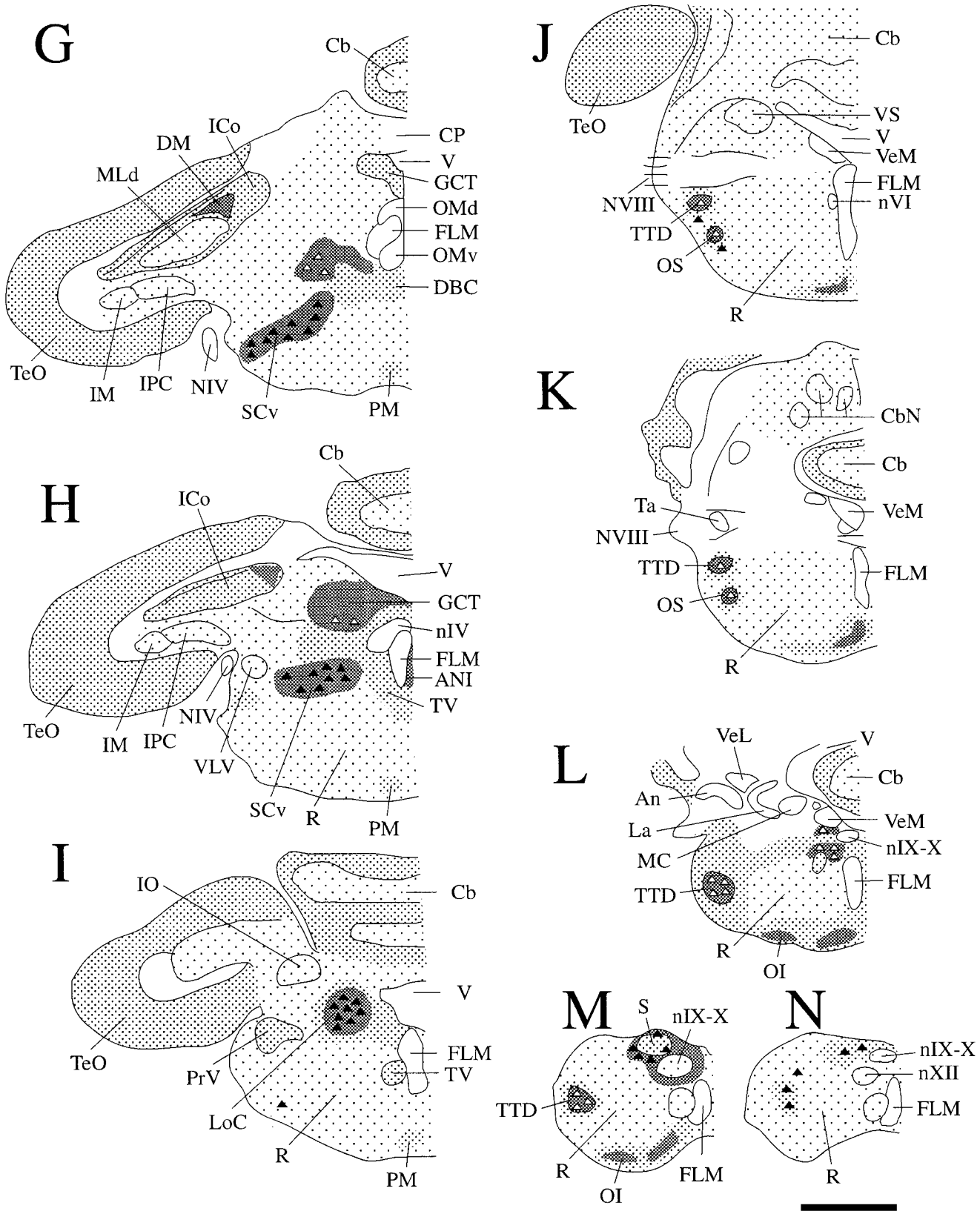

Figure 2 (Continued)

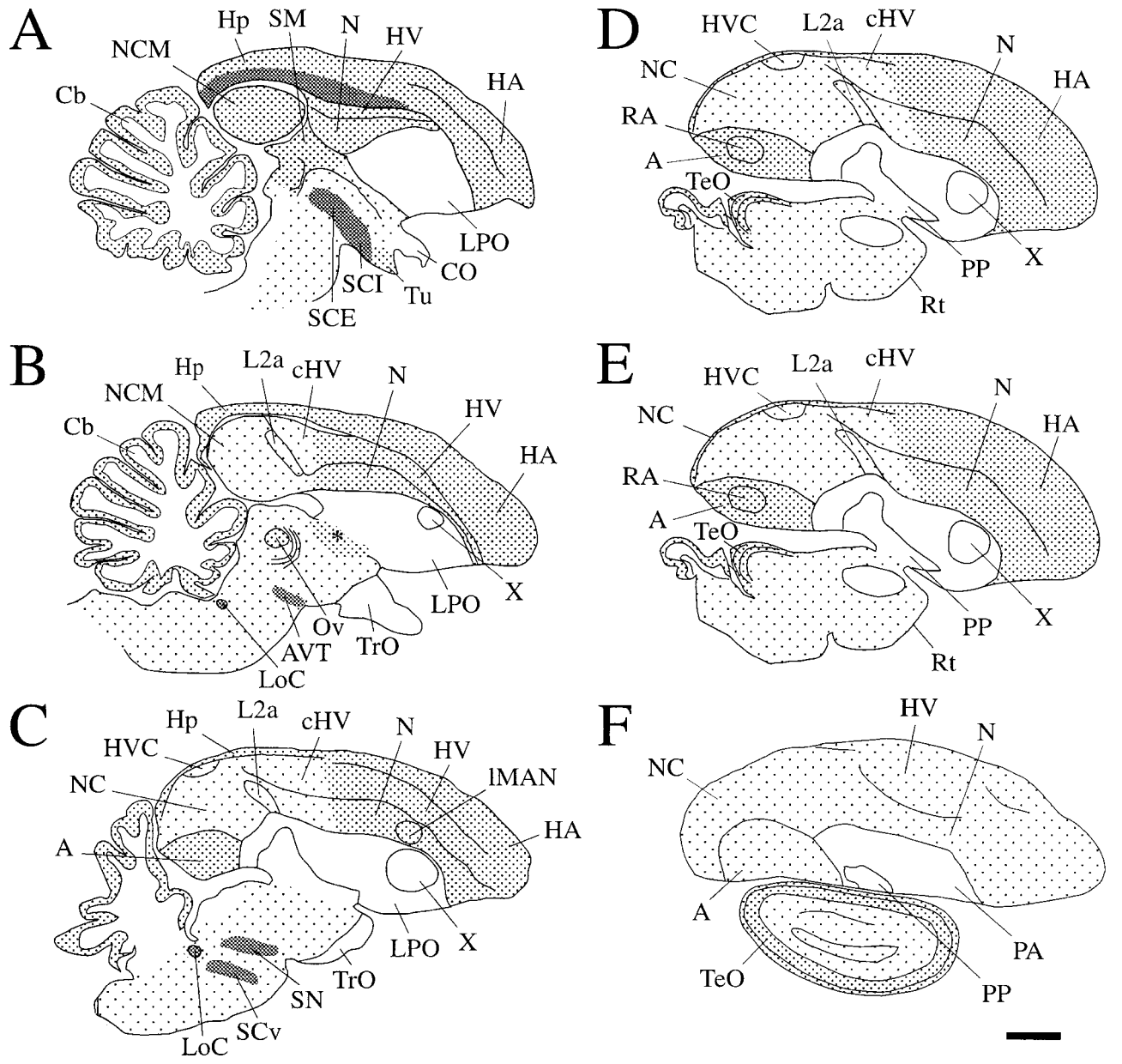

Fig. 3. **A–F:** Maps of the distribution of DBH-ir in the zebra finch telencephalon. The distinct patterns of DBH-ir (for keys, see Fig. 1) were mapped onto camera lucida drawings of a series of parasagittal sections. Only a few structures in the diencephalon, brainstem, and lower regions are shown (these regions are detailed further in Fig. 2). In A–F, the planes correspond, respectively, to parasagittal planes at 0.3, 1.0, 1.8, 2.1, 2.4, and 3.0 mm from the midline. The area in the basal forebrain indicated by an asterisk in B is shown in detail in a frontal section in Figure 8A. Solid triangles represent labeled somata. For other conventions, see Figure 2. Orientation: for this and all other figures derived from parasagittal sections, dorsal is up and anterior to the right. For abbreviations, see list. Scale bar = 1 mm.

thearchistriatum, the fibers had a more reticular appearance (see below). Next, in terms of density, came the caudal and lateral portions of the neostriatum and of all subdivisions of the hyperstriatum, which had moderate levels of DBH-ir (Fig. 3B–F). It is in these regions that most of the telencephalic auditory processing areas as well as song control nuclei are situated. These two groups are described separately below.

Auditory regions. Field L and the caudomedial neostriatum (NCM) had comparable densities of DBH-labeled fibers and varicosities, which were somewhat higher medially and tended to decrease more laterally (Fig. 3B–E; for detail of NCM, see Fig. 1B). All field L subdivisions (L1, L2a,b, and L3) shared a similar density of immunoreactivity (Fig. 6). This contrasted with the absence of staining seen in the adjacent caudodorsal paleostriatum (Pc; Fig. 6), an area that appears to receive a direct projection from the auditory thalamus (Kelley and Nottebohm, 1979; Wild et al., 1993; Vates et al., 1996). A moderate density of DBH-ir was seen throughout most of the mediolateral extent of the caudal hyperstriatum ventrale (cHV; Fig. 3B–E), an auditory station that is interconnected highly

with field L and the NCM. The auditory shelf region under the song nucleus HVC also had a moderate density of immunoreactive fibers (Figs. 3C–E, 7A), which tended to be aligned along the rostrocaudal axis in a disposition reminiscent of that of fibers seen in tract-tracing studies of this area (Vates et al., 1996; Mello et al., 1998). One of the highest densities of DBH staining within the auditory system was seen in the archistriatal tissue that surrounds the song nucleus RA, i.e., the RA cup (Figs. 3D, 7B).

Song control nuclei. All telencephalic song control nuclei were characterized by a low to moderately high degree of immunoreactivity, and none stood out from the surrounding areas. Rather, the density of their innervation reflected that of their surroundings. Within the HVC, DBH-labeled fibers usually had an orientation perpendicular to those within the shelf region (Fig. 7A). It is possible that these fibers were direct branches from the shelf fibers. This could not be determined, however, because the labeled fibers appeared only as short segments that could not be followed for very long distances. Often, we could see fine ramifications containing numerous varicosities and granulations, indicative of terminal branching (not shown). Within the nucleus RA, the fibers had a reticular appearance typical of the archistriatum (Figs. 3D,E, 7B). A fairly high innervation by DBH-ir elements characterized lMAN (Figs. 3C, 7C), where large, unstained cell bodies were surrounded by immunoreactive ramifications and varicosities, forming a fine net of branching processes. A low-to-moderate innervation, reflecting the staining levels of the adjacent auditory neostriatum, was seen in the nucleus interfascialis (NIf; not shown).

Paleostriatum. A marked feature of the DBH immunostaining pattern in the telencephalon was the almost complete absence of immunoreactive elements within the paleostriatum (Fig. 3A–F), including most of the lobus paraolfactorius (LPO), song nucleus area X, the paleostriatum augmentatum (PA), the auditory Pc (Fig. 6), and most of the paleostriatum primitivum (PP). Only occasionally did we find a few isolated fibers within the paleostriatum; these were mostly devoid of varicosities or branching and may represent fibers of passage (Fig. 1A). There was one exception: An area of high labeling intensity was seen in the transition zone between the ventromedial portion of the LPO and the septum (Se), close to the ventral tip of the lateral ventricle and the nucleus accumbens. In the series of frontal sections, this labeled field extended rostrocaudally from the level of the tractus septomesencephalicus (TrSM) to that of the anterior commissure (see area indicated by asterisks in Figs. 2A–C, 3B, 8A).

Septum. For the septum and the remaining brain subdivisions, our analysis was based mostly on the series of frontal sections. The septum, including the medial and lateral septal nuclei, showed a moderate-to-high density of immunoreactive elements, consisting of a dense array of highly branched fibers with numerous varicosities (Figs. 2A–C, 8B). A particularly high density of DBH-ir was seen in a small nucleus in the ventromedial septum dorsal to the anterior commissure, the nucleus commissuralis septi (CoS; Figs. 2C, 9A). The main fiber tract within the septal area, the TrSM, was devoid of labeled fibers (Fig. 2A, 8A).

Diencephalon. In the preoptic area, particularly high densities of DBH-ir were seen in the area that included the POM (Figs. 2A–C, 9A). The highest innervation density occurred along the periventricular region, including the medial portion of the POM, whereas a lower density was seen in more lateral portions of this nucleus. One of the highest densities of DBH-ir in the diencephalon (and even in the whole brain) was seen ventromedial to the POM in the PVN (Figs. 2B,C, 9A–C); this nucleus contained numerous DBH-positive elements that consisted mostly of terminal branches, varicosities, and granulations surrounding the large, negative perikarya characteristic of the PVN (Fig. 9B). The lateral portion of the rostral hypothalamus (LHy) had a fairly high innervation in contrast to a somewhat sparser density in the area that included the nucleus ventromedials hypothalami (VMN; Fig. 2B). Very high densities of DBH-ir were also seen in the stratum cellulare externum (SCE) and internum (SCI) and in the medial tuberal region (Figs. 2C, 9C); dense pericellular arrangements could be seen in all of these areas (Fig. 2C; for detail, see Fig. 9D) as well as in the region that immediately preceded the SCE and SCI (Fig. 2B).

Moderate levels of DBH-ir were seen in the epithalamus, including the medial and lateral habenular nuclei (Fig. 2E). The thalamus was generally characterized by a scarce-to-moderate density of innervation. A high density of DBH-ir elements was seen only in the nucleus paramedianus internis (PMI; Fig. 2D). A moderate density was seen in the auditory nucleus ovoidalis (Ov; Figs. 2C–E, 10), in the surrounding tissue that constitutes the Ov shell (Durand et al., 1992; Vates et al., 1996), and along the tractus ovoidalis (tOv), which carries the Ov afferents from the auditory midbrain (Fig. 2D). A low density of DBH-ir was seen in medial thalamic nuclei, including the posterior nucleus of the dorsomedial thalamus (DMP) and the dorsointermediate nucleus of the posterior thalamus (DIP) as well as the nucleus spiriformis medialis (SPM); whereas, in most other thalamic areas, DBH-ir was either scarce—as in the visual nucleus rotundus (Rt) and the nuclei of the ventrolateral thalamus, including the nucleus geniculatus lateralis, pars ventralis (GLV), the nucleus ventrolateralis thalami (VLT), and the nucleus posteroventralis thalami (PV), or it was negligible, as in the DLM and the nuclei dorsolateralis posterior thalami (DLP), spiriformis lateralis (SPL), pretectalis (Pt), and uvaeformis (Uva), and the area pretectalis (Fig. 2C–F). A slightly higher density was seen in the interstitial space surrounding most of these thalamic nuclei.

Mesencephalon. A moderate-to-high density of DBH-ir was observed throughout several portions of the mesencephalon. Within the rostral mesencephalon, a densely labeled field was seen immediately lateral to the emergence of the oculomotor nerve (NIII), containing numerous labeled fibers and varicosities arranged in an intricate termination bed (Figs. 2D, 11A). This location corresponded to the area ventralis of Tsai (AVT). More caudally, labeled fibers in AVT accompanied the fibers of NIII as they moved dorsally and occupied a gradually broader area (Fig. 2E). At this level, another comparably dense termination bed was seen in a separate field lateral to AVT and corresponding to SN (Figs. 2E,F, 11B). SN contained numerous DBH-ir elements, particularly fibers and varicosities covering negative perikarya and dendritic processes (Fig. 11C). The fields of labeled fibers in SN and AVT then merged at a slightly more caudal level to form a large region of dense DBH-ir in the central portion of the tegmentum (Fig. 2F,G) ventrolateral to the anterior oculomotor complex and the fasciculus longitudinalis medialis (FLM). Farther caudally, this zone became less dense and moved dorsally, coming to occupy a position immediately

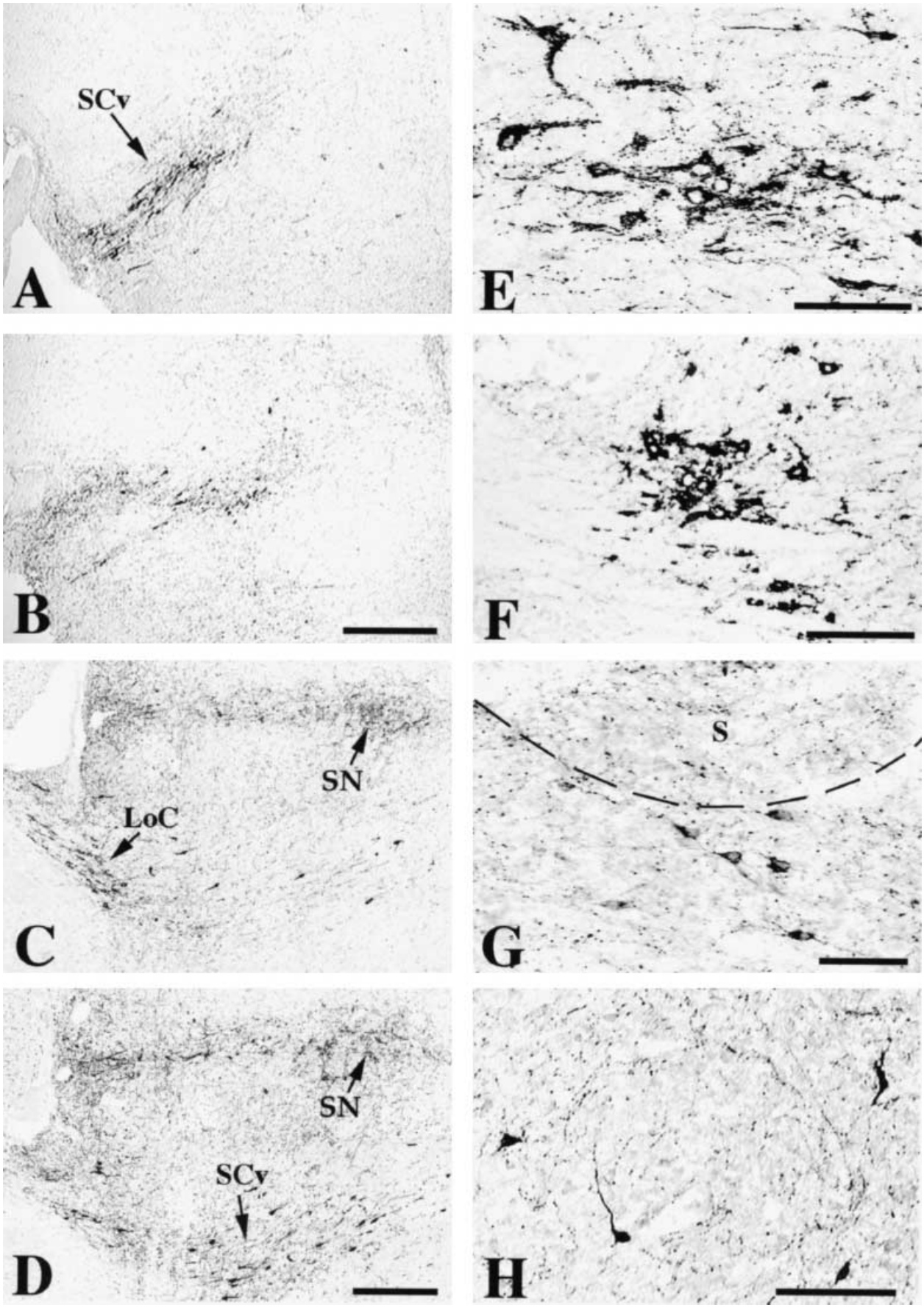

Figure 4

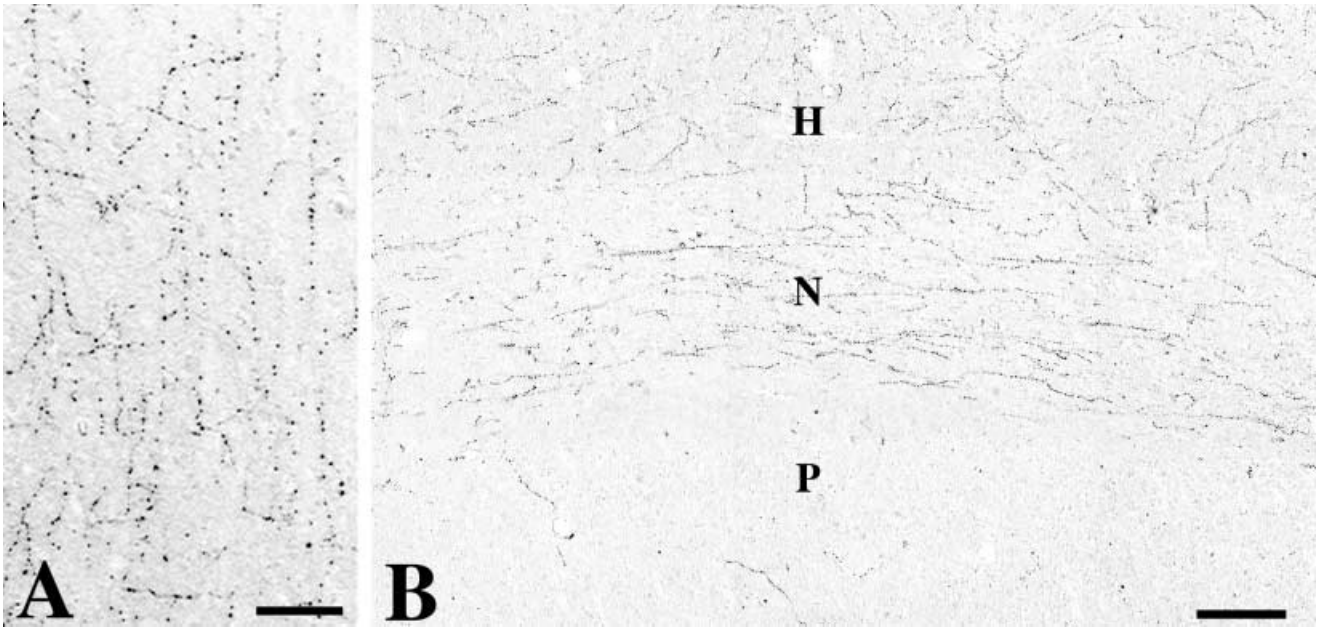

Fig. 5. Photomicrographs depicting DBH-ir elements in the medial telencephalon in a parasagittal section (at the level of panel A in Fig. 3). Panel A: Detailed view of DBH-labeled fibers and varicosities in the ventromedial hippocampus; notice that the majority of fibers assume a vertical orientation, as they ascend from the septal region, in contrast to the more reticular appearance of DBH-ir elements at more dorsolateral levels of the hippocampus (as detailed in Fig. 1D). Panel B: Notice the preferential dorsocaudal orientation of DBH-labeled fibers in the N, as opposed to the more reticular appearance in H and scarcity of DBH-ir elements in P. Scale bar = 100 μm in A, 200 μm in B.

lateral to nIV and continuous with the fiber-rich zone surrounding the LoC.

A somewhat lower density of innervation could be seen in some portions of the ventral mesencephalon, including the nuclei interpeduncularis (IP) and mesencephalicus profundus ventralis (MPv; Fig. 2E,F), and dorsally in the substantia grisea centralis (GCT; Figs. 2G, 12A). In contrast, DBH-ir was low or scarce in the Edinger-Westphal nucleus (not shown) and practically absent in other nuclei of the anterior oculomotor complex, including nuclei nervi oculomotorii, pars ventralis (OMv) and dorsalis (OMd; Figs. 2G, 12C). Several fibers were seen coursing along the pretectal area toward the posterior commissure, which they seem to cross (Figs. 2G, 12B). Other fibers traveled toward the optic tectum, which had a moderate-to-high density of innervation (Fig. 2B–J). The highest densities of

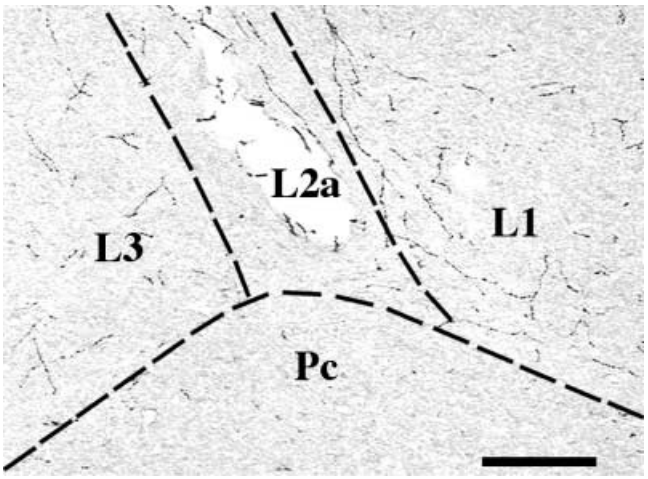

Fig. 6. Photomicrograph depicting DBH-ir elements in auditory field L in a parasagittal section (at the level of Fig. 3C). Note a similar low density of labeled fibers in all subfields shown (subdivisions L1, L2a, and L3 of field L) in contrast to the absence of immunoreactivity in the caudodorsal paleostriatum (Pc). Dashed lines are drawn over the subfield boundaries. Scale bar = 100 μm.

DBH-ir were seen in the strata griseum et fibrosum superficiale (SGF) and griseum centrale (SGC), whereas the strata album centrale (SAC) and opticum (SOp) had scarce innervation (Fig. 13A), and the nuclei isthmi, pars parvocellularis (IPC) and magnocellularis (IM) and semilunaris (SLu), showed a moderate density of DBH-ir (Fig. 2D–H). Within the torus semicircularis (ToS), a high density of DBH-ir was seen in the ICo, particularly within DM (Figs. 2G, 13B), a nucleus in the motor pathway for

Fig. 4. Photomicrographs depicting DBH-positive cell bodies in the zebra finch brain. **A,B**: Frontal sections (same levels shown in Fig. 2G,H) showing labeled cells in the SCv. Note that these are displaced dorsomedially at the more caudal level. **C,D:** Parasagittal sections (at levels slightly medial and slightly lateral to that shown in Fig. 3C) showing labeled cells in the LoC and the SCv and labeled fibers in the SN. **E:** Detail of labeled somata in the SCv. Note the large, darkly stained, triangular cell bodies and the unstained nuclei. **F:** Detail of labeled somata in the LoC. Note the darkly stained, round or oval-shaped cell bodies and the unstained nuclei. **G:** Detail of labeled somata in the vicinity of S (at the level of Fig. 2M). Note that cells are small and triangular or round shaped, with weaker cytoplasmic staining than in the LoC and the SCv. The dashed line represents the boundary of S as seen in Nissl-stained sections. **H:** Detail of scattered, labeled cell somata in the caudolateral medulla (at the level of Fig. 2N). Note the irregularly shaped cells with darkly stained perikarya and dendritic processes. For abbreviations, see list. Scale bars = 400 μm in A,B, 300 μm in C,D, 50 μm in E–H.

song control. In fact, DM was the song control nucleus that showed the highest density of DBH staining, which consisted mostly of highly branching terminal ramifications with numerous varicosities as well as numerous negative cell bodies covered with a very high density of immunopositive granules and varicosities (Fig. 13C). A moderate innervation was seen within the auditory nucleus mesencephalicus lateralis, pars dorsalis (MLd) and the immediately surrounding area (Figs. 2F,G, 13B).

At the level of the caudal mesencephalon, nIV stood out as a nucleus that basically was devoid of fibers (Figs. 2H, 12E), in sharp contrast to a very high density within a small zone that contours FLM ventromedially and that corresponds to the location of the nucleus anularis (ANI; Figs. 2H, 12C–E). A very high density was also seen in the caudal GCT region that precedes the field of labeled perikarya within LoC (Figs. 2H, 12F). High densities were also seen immediately ventrolateral to FLM in the area occupied by the nucleus tegmenti ventralis (TV) and farther ventrolaterally in association with the labeled perikarya in the SCv (Fig. 2H). A moderately high density of DBH-ir could be seen in a ventromedial region that contains the rostral portion of the nucleus pontis medialis (PM; Fig. 2G). Otherwise, a low density of punctate immunolabeling could be seen throughout the whole mesencephalon and pontine mesencephalic transition (Fig. 2E–I).

Pons, medulla, and cerebellum. The level immediately caudal to the nIV was dominated by the immunopositive cell bodies in the LoC (Figs. 2I, 4F). The separate fields of labeled fibers seen at more rostral levels in the GCT, LoC, and SCv merged at this level to form one continuous field of dense DBH-ir that surrounded the immunopositive cells in the locus coeruleus (Fig. 2I). In the dorsolateral portion of the pons, a moderately high concentration of DBH-ir was observed in association with the principal sensory nucleus of the trigeminal nerve (PrV; Fig. 2I). In contrast, a low density of innervation was observed slightly more rostrally, in the area where the lateral lemniscus and associated nuclei are located (Fig. 2H). At more caudal levels of the pons, DBH-ir predominated in the ventrolateral portion, with fairly high densities seen in the superior olive (OS) and the nucleus and tractus descendis nervi trigemini (TTD; Fig. 2J,K), with the latter containing a high number of dense pericellular arrangements of DBH-ir elements (Fig. 14A). Moderate-to-dense levels of DBH-ir were seen ventromedially in the PM (Fig. 2G–I), whereas little innervation characterized most of the reticular formation (R). DBH-ir elements were practically absent from most of the dorsal pons, including the lateral, superior, and medial nuclei of the vestibular complex (VeL, VS, and VeM, respectively) and, farther caudally, the auditory angular, laminar, and magnocellular nuclei (An, La and MC, respectively; Fig. 2J–L).

In the rostral medulla, dense beds of DBH-ir were seen ventrally and ventromedially in the inferior olive and surroundings as well as laterally in the medullary portion of the TTD (Fig. 2L,M). A high density was also seen dorsomedially in the region that surrounds nIX–X (Figs. 2L–N, 14B) and S (Fig. 2M). In the two latter structures, most of the DBH-ir was seen outside the nuclei in association with the labeled perikarya seen in these areas, although a significant bed of DBH-ir elements was also seen within S. A low-to-moderate innervation was seen throughout most of the reticular formation at all rostrocaudal levels of the medulla (Fig. 2L–N).

A moderate-to-high density of DBH-ir could be found throughout the entire cerebellar cortex (Figs. 2, 3), with a slight predominance of granular over Purkinje and molecular cell layers (Fig. 14C). Some variability in the local density was seen across different cortical regions; little staining was seen within deep cerebellar nuclei.

DISCUSSION

Methodological issues

We used a polyclonal rabbit antibovine-DBH antiserum of commercial origin and well-established specificity in both mammals and birds; the same antiserum was used previously to investigate the noradrenergic system in the chicken brain (Moons et al., 1995). Similarly, an antibovine DBH from a different source was used to study the quail brain (Bailhache and Balthazart, 1993). The overall similarities between the immunostaining patterns we obtained and those seen in the previous studies mentioned above, as well as those seen in studies of the pigeon (Reiner et al., 1994), give strong indication that the anti-DBH antiserum we used recognizes the same antigen in zebra finches as in other avian species.

Whereas TH is expressed in all catecholaminergic cells, DBH is the key enzyme in the conversion of dopamine to noradrenaline and is absent in dopaminergic cells. Therefore, a comparison between the staining patterns obtained with anti-DBH and anti-TH antisera, in principle, should allow differentiation between the dopaminergic and noradrenergic systems by subtraction (for discussion, see below). However, DBH is expressed in both cells that synthesize noradrenaline and adrenaline, and its detection does not differentiate between noradrenergic and adrenergic cells. Current evidence derived from ICC studies by using antisera against phenylethanolamine-N-methyltransferase, the enzyme responsible for the conversion of noradrenaline to adrenaline, indicates that the presence of adrenergic cells is restricted to the medulla in the brains of both mammals (Tillet, 1988) and birds (Steeves et al., 1987; Reiner et al., 1994). Thus, although the DBH-positive cell bodies we observed in the caudal mesencephalon and pons are most probably noradrenergic, the possibility remains that at least some of the labeled cell groups in the medulla are adrenergic in nature (for further discussions, see Bailhache and Balthazart, 1993; Reiner et al., 1994).

Fig. 7. Detailed photomicrographic views depicting noradrenergic innervation of telencephalic song control nuclei in parasagittal sections. **A:** DBH-ir elements in the high vocal center (HVC) and its vicinity (at the level of Fig. 3D). Note the low-to-moderate density of labeled fibers and varicosities in both the HVC and the adjacent shelf region (Sh). **B:** DBH-ir elements in the robust nucleus of the archistriatum (RA) and surroundings (at the level of Fig. 3D). Note the moderately high density of labeled fibers and varicosities in the RA and the surrounding cup region, particularly in the rostroventral cup (indicated by asterisk). **C:** DBH-ir elements in the lateral magnocellular nucleus of the anterior neostriatum (lMAN) and surroundings (at the level of Fig. 3C). Note the moderately high density of fibers and varicosities, reflecting the corresponding density in the surrounding neostriatum (N). Dashed lines are drawn over telencephalic lamina and the boundaries of song nuclei as they appear after cresyl violet staining. For abbreviations, see list. Scale bar = 200 μm.

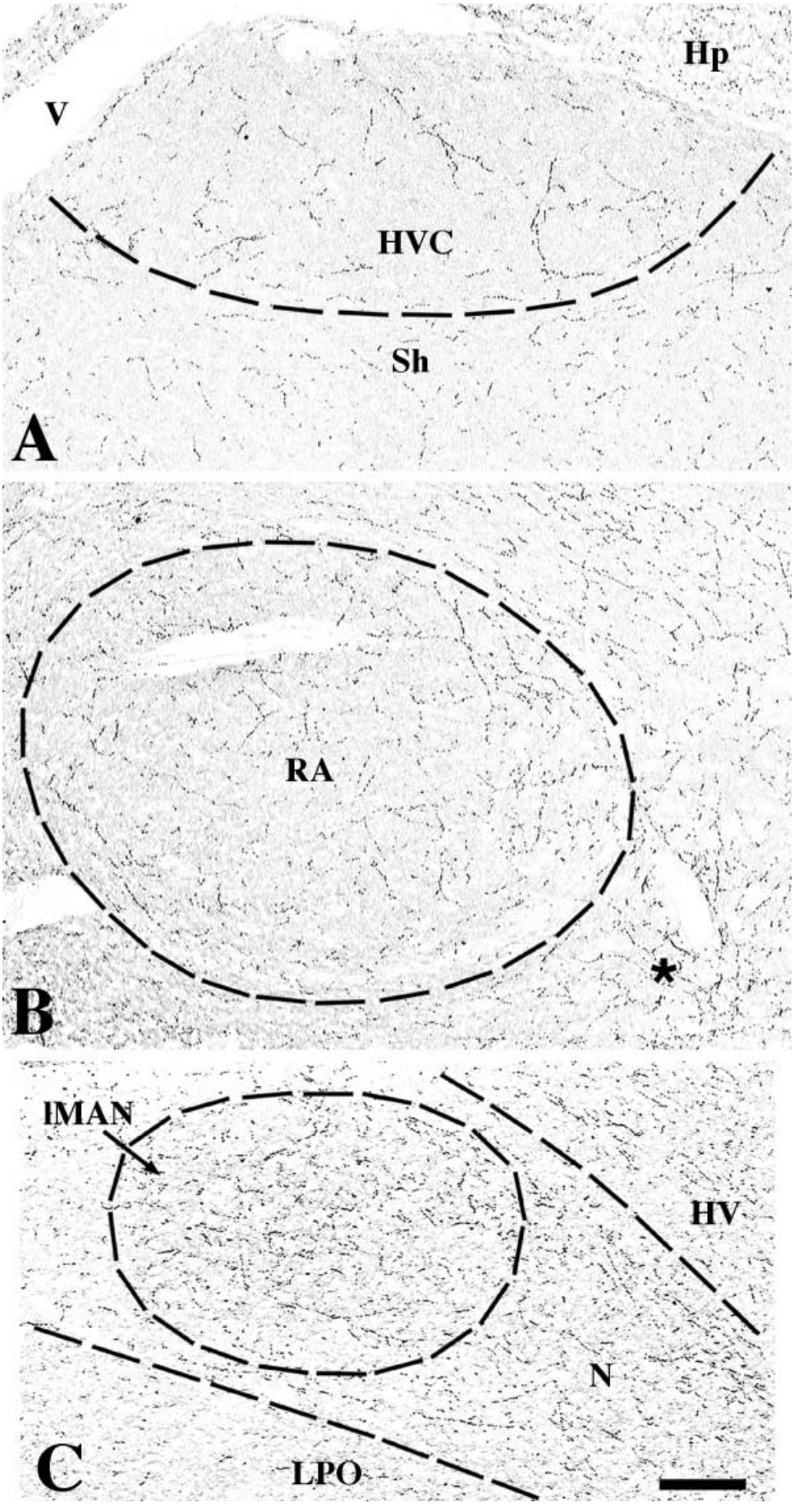

Figure 7

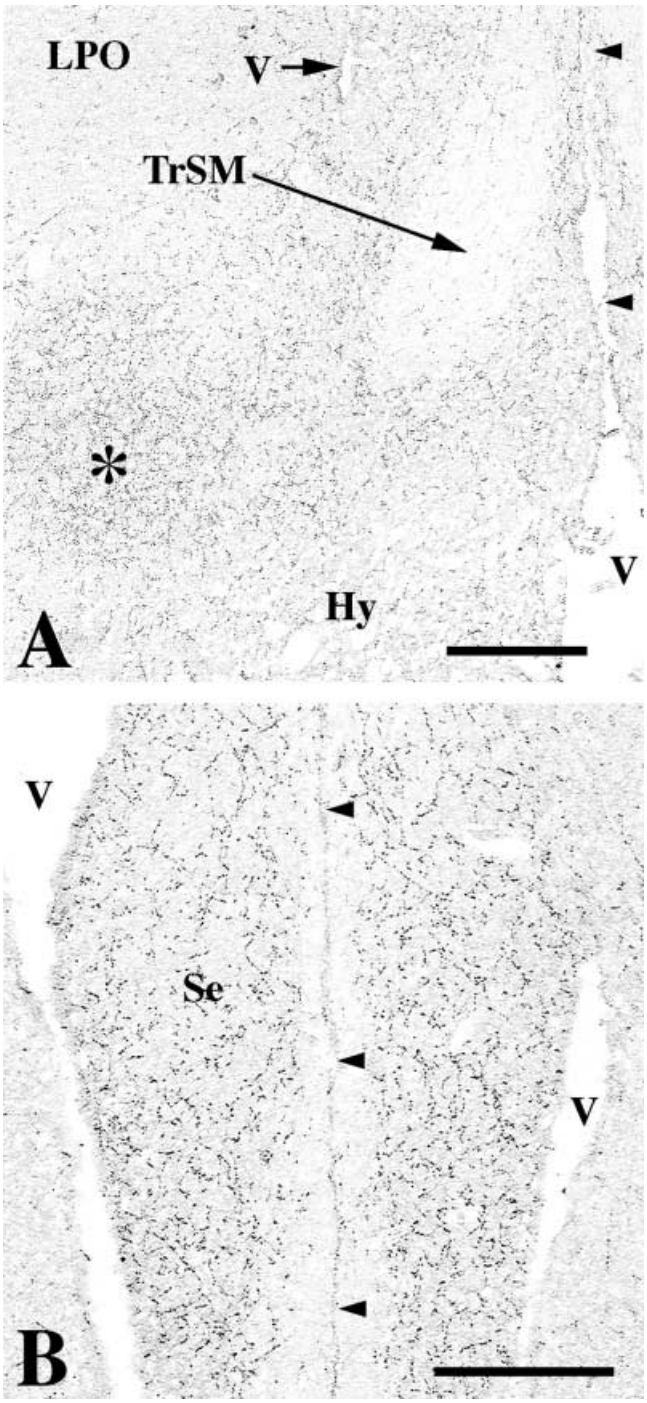

Fig. 8. Photomicrographs depicting the distribution of DBH-ir in the basal forebrain and septum in frontal sections. **A:** Photomicrograph corresponding to a plane slightly rostral to that shown in Figure 2A. Note the lack of staining in the septomesencephalic tract (TrSM) and the dense accumulation of DBH-ir elements in the ventromedial paraolfactory lobe (LPO; indicated by an asterisk) in the vicinity of the TrSM and dorsal hypothalamus (Hy). **B:** Photomicrograph from the same level shown in Figure 2A showing the relatively high density of fibers and varicosities in the rostral septal region. Arrowheads indicate the midline. For abbreviations, see list. Scale bars = 300 μm.

An interesting observation is that our use of parasagittal sections allowed a better and more complete visualization of DBH-ir in the telencephalon compared with the series of frontal sections. This is explained most probably by the fact that large numbers of DBH-positive fibers in the telencephalon, particularly close to the midline, are oriented along the rostrocaudal axis and are seen as punctate staining in frontal sections. Most of our analysis of DBH-ir in the telencephalon, therefore, was performed by using the series of parasagittal sections.

Finally, the abundance and wide distribution of DBH-ir elements in the brain make it extremely hard to determine and discriminate clearly the individual noradrenergic pathways and projections by using ICC methods alone. To address connectivity questions, such as the specific source of noradrenergic/dopaminergic projections to a discrete song control nucleus, such as the HVC, one needs to use anterograde and retrograde tract-tracing techniques, which are beyond the scope of the present analysis.

Comparisons with staining patterns in nonoscines

The general distribution of DBH-ir in the zebra finch brain was largely comparable to the patterns seen in previous studies that mapped the noradrenergic system in nonoscine avian species (Bailhache and Balthazart, 1993; Reiner et al., 1994; Moons et al., 1995). In both oscines and nonoscines, labeled somata are confined to structures in the caudal midbrain, pons, and medulla (mainly the LoC, SCv, OS, and S), whereas labeled fibers have a much broader distribution throughout most of the brain. Another distinctive feature of both groups is the presence of dense pericellular arrangements of strongly labeled DBH-ir elements surrounding immunonegative cell bodies in several brain structures along the rostrocaudal axis, particularly in the hypothalamus, midbrain, and pons.

The nomenclature adapted from the mammalian literature (Hökfelt et al., 1984) has provided a useful framework for describing catecholaminergic cell groups in the avian brain (for a detailed discussion, see Reiner et al., 1994). According to that scheme, the labeled somata observed along the rostrocaudal axis of the zebra finch brain would correspond to noradrenergic cell groups A6 (LoC and SCv), A5 (vicinity of OS), A4 (vicinity of VeM), A2 (S and vicinity) and A1 (lateral reticular formation). Labeled somata corresponding to cell groups A7 (lateral pons dorsal to SCv) and A3 (vicinity of inferior olive) were not observed, as was also described for nonoscines (Reiner et al., 1994). Finally, some of the DBH-labeled cells in S and in the lateral reticular formation may represent adrenergic cell groups C2 and C1, which intermingle with noradrenergic groups A2 and A1, respectively.

However, there are some discrepancies between the pattern we report here and the patterns described previously. For instance, the labeled cell bodies we observed in the ventrolateral medulla did not appear to be confined to the nucleus reticularis subtrigeminalis (RST), as described in the chicken (Moons et al., 1995) and the pigeon (Reiner et al., 1994), but, rather, to extend to the TTD. We also observed scattered labeled cells in the caudalmost portions of the medulla, possibly extending to the rostral cervical spinal cord; the previous studies of the chicken and pigeon brains may not have extended that far caudally. Similarly, some DBH-labeled cells in the SCv of zebra finches appear to extend farther rostrally than in the

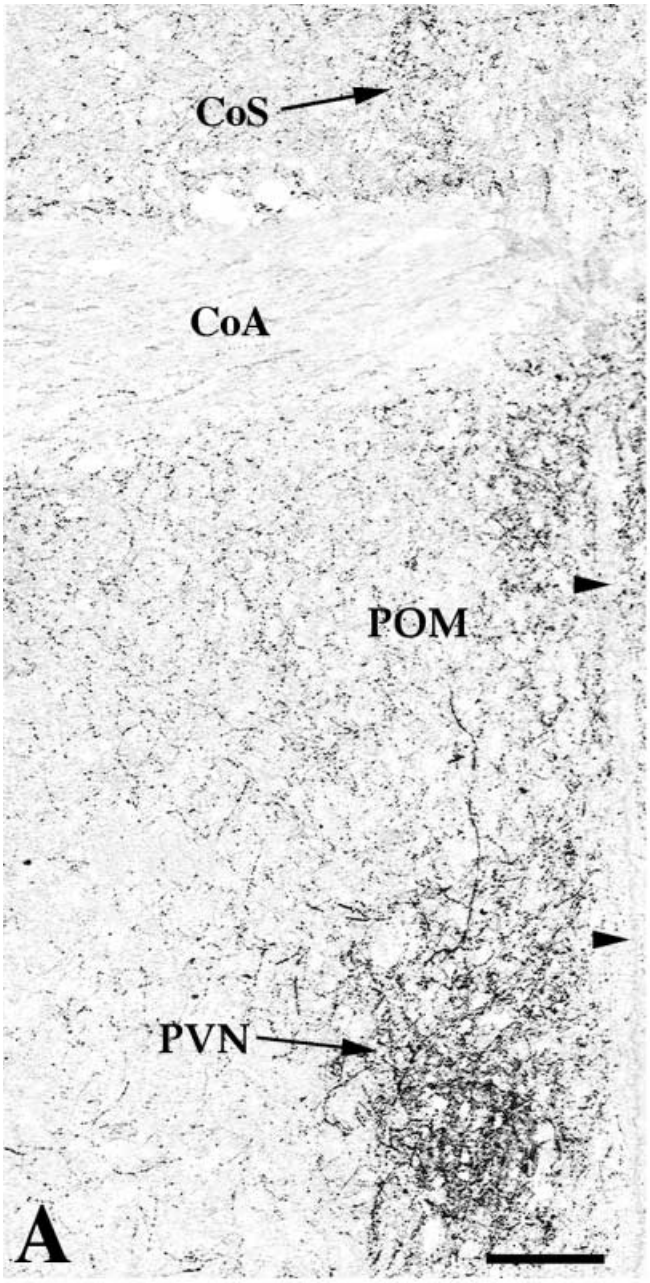

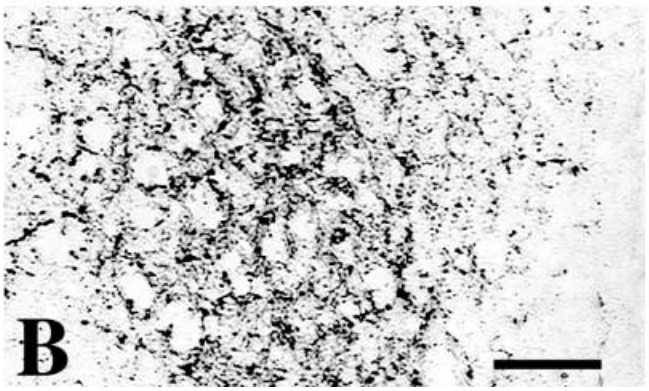

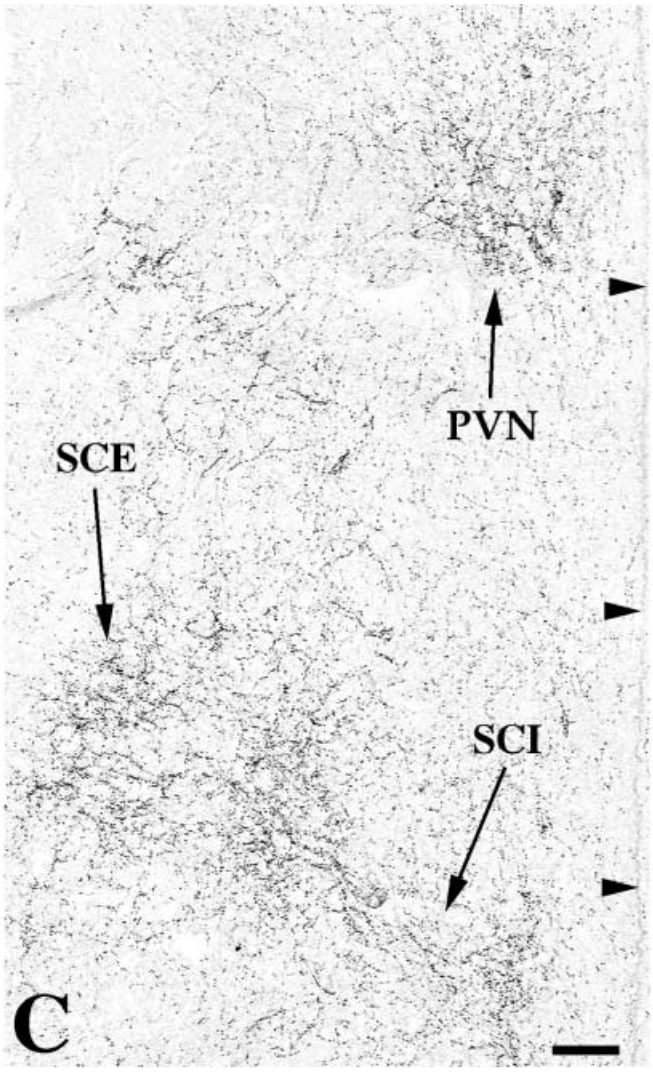

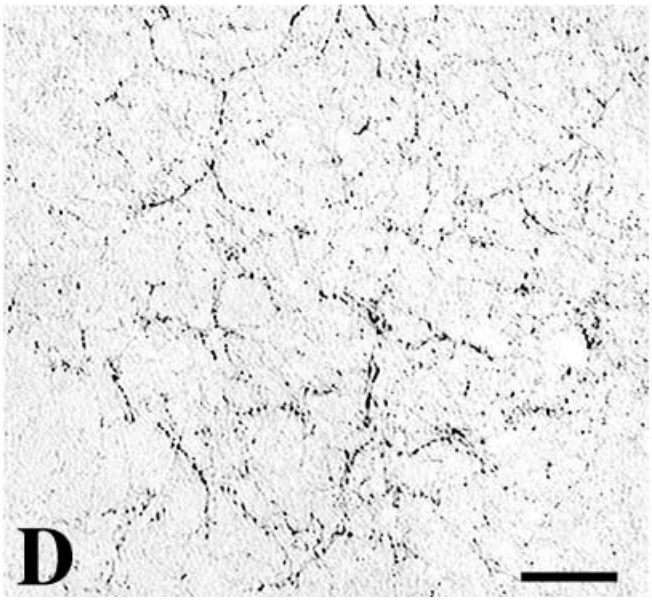

Fig. 9. Photomicrographs depicting the distribution of DBH-ir in the hypothalamus and ventrocaudal septum in a frontal section at the level of the anterior commissure (CoA; same plane shown in Fig. 2C). **A:** View of the dorsal hypothalamus. Note the very high density of DBH-labeled fibers and varicosities in the nucleus paraventricularis magnocellularis (PVN), the medial POM, and the nucleus commissuralis septi (CoS); the moderate-to-high density throughout the rest of the hypothalamus; and the lack of staining in the CoA. **B:** Detailed view of the pericellular arrangements of strongly labeled DBH-ir elements surrounding negative perikarya in the PVN. **C:** View of the middle hypothalamic region. Note the high density of DBH-labeled elements in the external and internal stratum cellulare (SCE and SCI, respectively) and in the PVN and the low-to-moderate levels in the surrounding hypothalamic regions. **D:** Detailed view of pericellular arrangements of DBH-labeled elements in the SCE. Arrowheads in A and C indicate the midline. For abbreviations, see list. Scale bars = 100 µm in A,C, 50 µm in B,D.

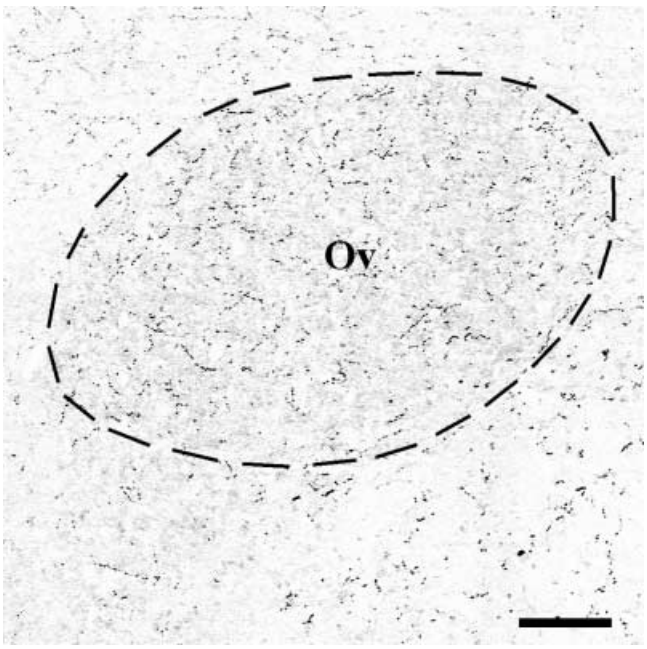

Fig. 10. Photomicrograph depicting DBH-ir elements within auditory thalamic nucleus ovoidalis (Ov) in a frontal section (the same level shown in Fig. 2E). Enclosed by the dashed line is an area that includes the Ov proper plus its immediately surrounding shell zone. Note the presence of a low-to-moderate density of DBH-stained elements consisting of short, fine processes and granulations. Scale bar = 100 μm.

chicken, possibly as far as the caudal reaches of the substantia nigra.

We also observed higher levels of DBH fiber labeling throughout the zebra finch brain than were reported previously for nonoscine avian species. In the telencephalon, this includes several regions in which DBH-ir had been described previously as scarce or absent in the quail, pigeon, and chicken, particularly in the neostriatal and hyperstriatal fields (Bailhache and Balthazart, 1993; Reiner et al., 1994; Moons et al., 1995). In the thalamus, the pattern observed bore a close resemblance to that described in the pigeon, with moderate staining in several nuclei located ventromedially, whereas little staining was reported in that area in the quail and chicken. These discrepancies suggest that there might exist species differences in the density of noradrenergic innervation, but they could also result partly from methodological differences, including sources of antisera, degrees of cross reactivity, and planes of brain sectioning. For instance, the studies of DBH distribution in nonoscines used frontal rather than parasagittal sections, which might render the visualization of stained fibers in the telencephalon more difficult (for discussion, see above).

DBH-ir in auditory processing areas

We observed a moderate but significant noradrenergic innervation in nuclei of the ascending auditory pathway, including the MLd, Ov, and field L, whereas such innervation was considered to be nonexistent in quail and chicken brains (Bailhache and Balthazart, 1993; Moons et al., 1995) and very scarce in pigeon brain (Reiner et al., 1994). This apparent difference could reflect a higher degree of noradrenergic influence on the auditory system in species in which vocal learning plays a central role, but quantitative analysis would be required to establish that point. Our findings also corroborate the biochemical detection of norepinephrine in auditory nuclei of zebra finches (Harding et al., 1998). The innervation observed in the primary auditory thalamorecipient zone (field L) and its adjacent targets, the NCM and the cHV, is of particular interest. The latter two regions present a robust gene-induction response when songbirds hear conspecific song (Mello and Clayton, 1994; Mello and Ribeiro, 1998), a phenomenon that could potentially be involved in long-term modification of neuronal properties and the laying down of song auditory memories (Chew et al., 1995). It is interesting to note that an intact locus coeruleus is necessary for gene induction in response to sensory stimulation in the mammalian brain (Cirelli et al., 1996). An intriguing possibility to be tested, therefore, is that the noradrenergic system is also necessary for song-induced gene induction in the NCM.

DBH-ir in song control nuclei

The immunostaining pattern for DBH allowed a separation of the song control nuclei into three categories: 1) immunopositive nuclei with a higher fiber density than the surrounding tissue (the only representative here is the mesencephalic nucleus DM, the song control nucleus that had the highest density of DBH-ir elements); 2) immunopositive nuclei with a fiber density comparable to that of the surrounding tissue (the majority of song nuclei fall into this category, including the HVC, RA, lMAN, NIf, DLM, and Uva; note that, for the latter two nuclei, DBH staining was low but detectable); and 3) nuclei in which no DBH immunostaining was observed (the sole representative of this category was area X of the paleostriatum). These results provide a direct demonstration of a noradrenergic innervation of the song control system, substantiating the previous biochemical detection of norepinephrine and the autoradiographic demonstration of adrenergic receptors in several song control nuclei (Barclay and Harding, 1988, 1990; Sakaguchi and Saito, 1989; Ball, 1990, 1994; Casto and Ball, 1996; Harding et al., 1998). It is interesting to note that one of the highest concentrations of norepinephrine within the song system occurs in the DM (Barclay and Harding, 1988, 1990), consistent with the high innervation density we observed in this nucleus. It is also of interest to note that, whereas several song nuclei (HVC, RA, MAN) have a higher density of alpha-2 adrenergic receptors than the surrounding tissues (Ball, 1990, 1994; Casto and Ball, 1996), their density of innervation by DBH fibers is not any higher than that in their surroundings. This receptor specialization may reflect a higher sensitivity of the song system to the action of norepinephrine. For the most part, our results are consistent with the view that the noradrenergic system plays an important role in the control of singing behavior (Barclay et al., 1992). The results are also compatible with the suggestion that modulation of norepinephrine levels within song control nuclei may be part of the mechanism(s) by which steroids modulate singing (Barclay and Harding, 1988, 1990; Barclay et al., 1992).

Intriguingly, our study provides no substantiation for a noradrenergic innervation of area X. This conflicts with the previously reported detection of norepinephrine and the demonstration of noradrenergic receptors in this song nucleus (Barclay and Harding, 1988, 1990; Ball, 1994; Ball et al., 1994; Casto and Ball, 1996; Harding et al., 1998).

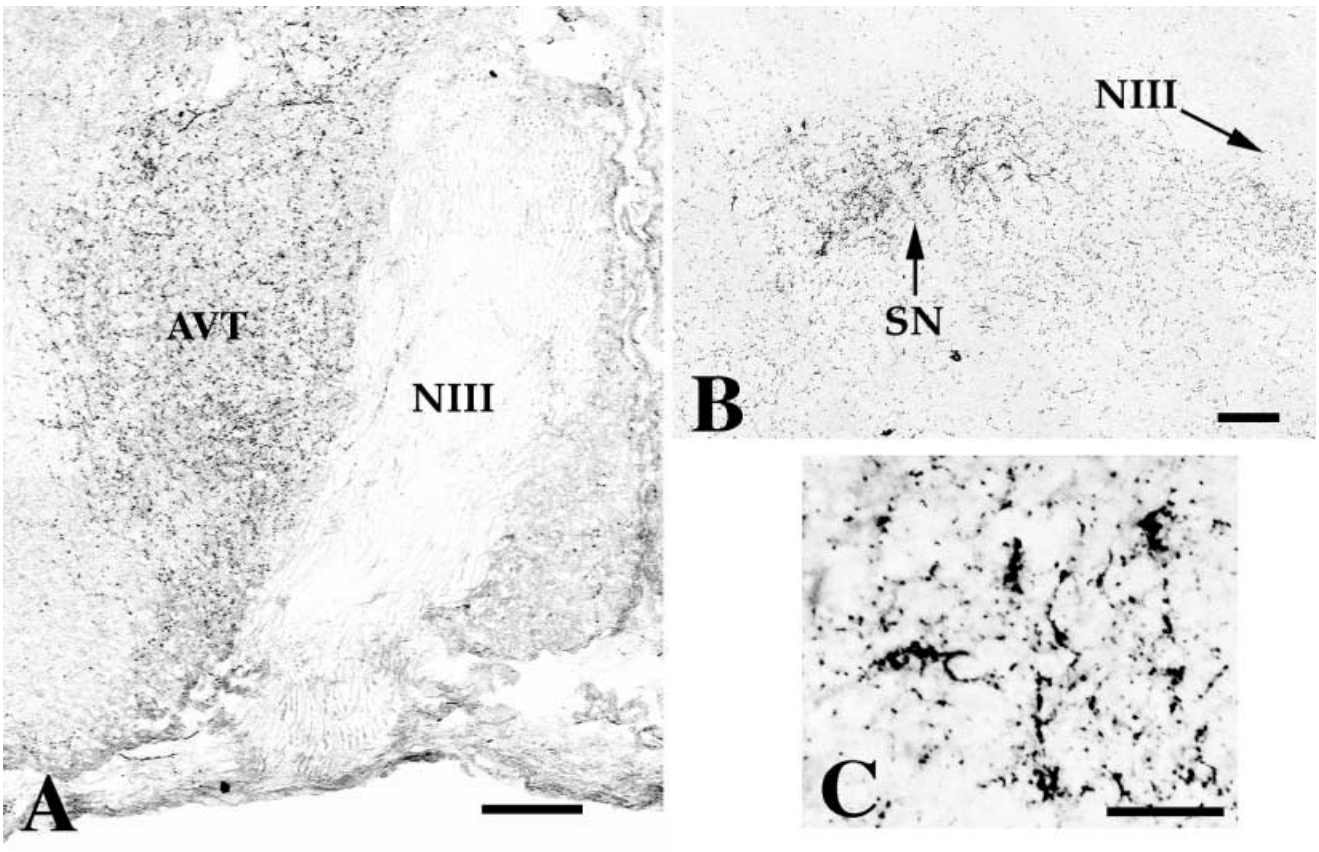

Fig. 11. **A–C:** Photomicrographs depicting noradrenergic innervation of the avian equivalent of the mammalian substantia nigra in frontal sections. A: View of the ventral tegmental area (same level shown in Fig. 2D). Note the high density of DBH-ir elements, consisting of fine terminal processes and varicosities, in the area ventralis of Tsai (AVT). B: View of the substantial nigra (SN) and surroundings (same level shown in Fig. 2F). Note the high density of DBH-ir elements in the SN, including several dense pericellular arrangements, which are shown in further detail in C. NIII, oculomotor nerve. Scale bars = 100 μm in A,B, 50 μm in C.

One possible explanation would be a low sensitivity of the anti-DBH antiserum used. Area X, however, together with the surrounding LPO and paleostriatum, was among the very few brain regions that was practically devoid of DBH-ir; this indicates that a noradrenergic innervation of these areas, if it is present, would probably be significantly lower than in most other brain regions. Also, the conspicuous absence of noradrenergic fibers in the LPO (area X included) and the paleostriatum, areas that are considered to be the avian equivalent of the mammalian caudate putamen, agrees well with the DBH-staining patterns described previously in other avian species (Bailhache and Balthazart, 1993; Reiner et al., 1994; Moons et al., 1995).

The apparent absence of DBH immunostaining in area X raises concern about the origins of the norepinephrine that was detected previously in this area. One possible explanation is that the samples utilized for biochemical measurements might have included material from adjacent regions, such as the rostral N, that is rich in DBH-labeled fibers. That would not explain, however, the high density of adrenergic receptors described for area X (Ball, 1994). Alternatively, noradrenaline might not be produced locally within area X but, rather, transported from other brain sites by as yet undetermined mechanisms. A more conservative explanation, however, is that DBH immunostaining does not reveal the full extent of the noradrenergic innervation. Antinoradrenaline antisera, as described in the chicken, yield a somewhat more detailed demonstration of the noradrenergic innervation than anti-DBH-antisera (Moons et al., 1995). Those authors argued that this may result from a higher accumulation of the transmitter in terminal arborizations and presynaptic terminals, whereas DBH-ir would be confined mostly to cell bodies, dendrites, and the largest axonal branches. The differences presented in that report between the two antisera were rather small, however, and it remains to be shown whether that explanation accounts for the lack of DBH staining in area X.

Comparison with TH distribution in oscines

Our description of the distribution of DBH-ir, as discussed above, provides a fairly complete picture of the noradrenergic system in the zebra finch brain. By applying the logic of subtraction to previous descriptions of TH-ir, it should be possible to determine the identity of dopaminergic elements. Such analysis should be performed with caution, however. Previous descriptions of the distribution of TH-ir in the zebra finch brain focused mainly on the song control system (Bottjer, 1993; Soha et al., 1996). It is therefore unclear whether structures that were not mentioned directly in those studies, such as specific nuclei in the thalamus and the midbrain, were actually devoid of

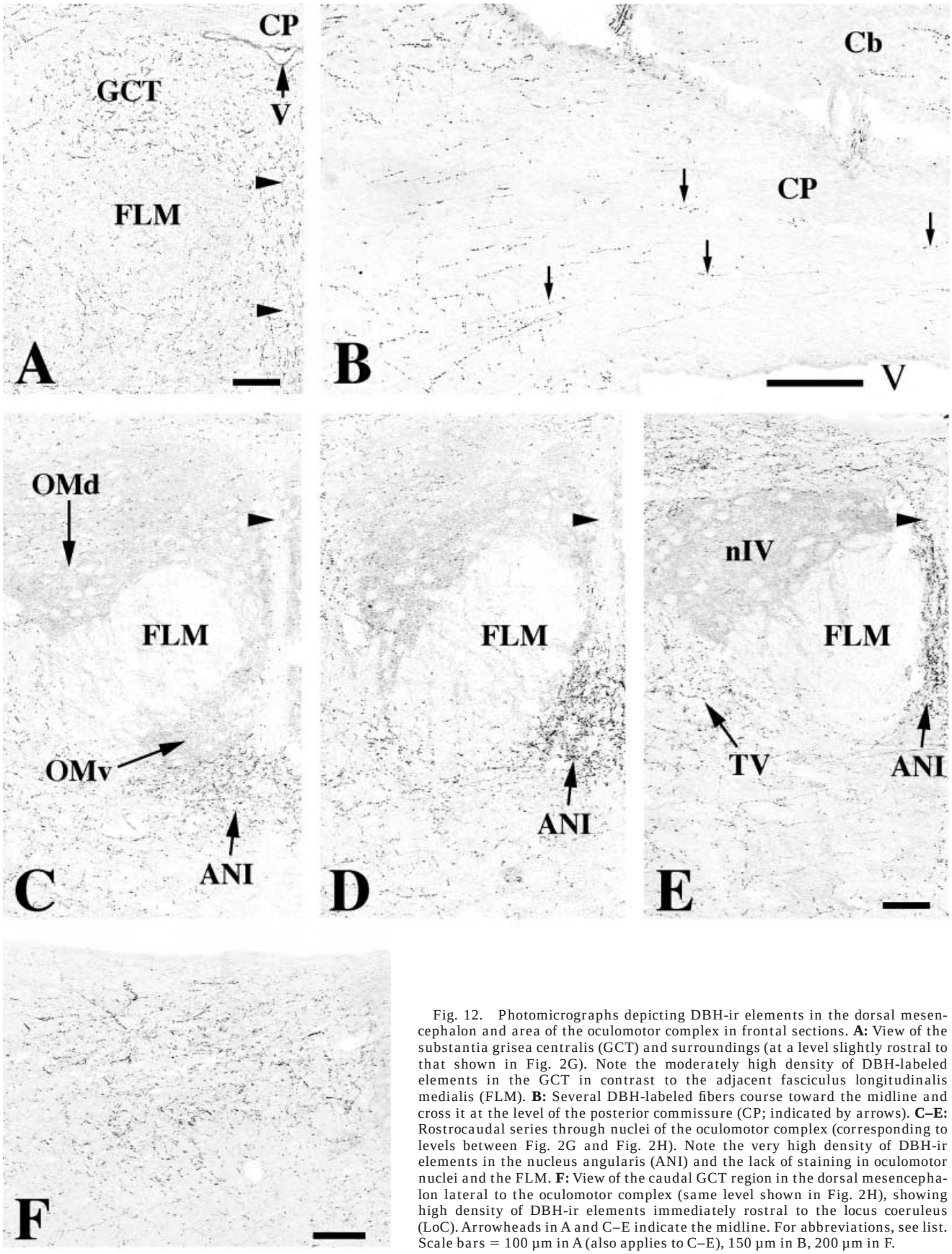

Fig. 12. Photomicrographs depicting DBH-ir elements in the dorsal mesencephalon and area of the oculomotor complex in frontal sections. **A:** View of the substantia grisea centralis (GCT) and surroundings (at a level slightly rostral to that shown in Fig. 2G). Note the moderately high density of DBH-labeled elements in the GCT in contrast to the adjacent fasciculus longitudinalis medialis (FLM). **B:** Several DBH-labeled fibers course toward the midline and cross it at the level of the posterior commissure (CP; indicated by arrows). **C–E:** Rostrocaudal series through nuclei of the oculomotor complex (corresponding to levels between Fig. 2G and Fig. 2H). Note the very high density of DBH-ir elements in the nucleus angularis (ANI) and the lack of staining in oculomotor nuclei and the FLM. **F:** View of the caudal GCT region in the dorsal mesencephalon lateral to the oculomotor complex (same level shown in Fig. 2H), showing high density of DBH-ir elements immediately rostral to the locus coeruleus (LoC). Arrowheads in A and C–E indicate the midline. For abbreviations, see list. Scale bars = 100 μm in A (also applies to C–E), 150 μm in B, 200 μm in F.

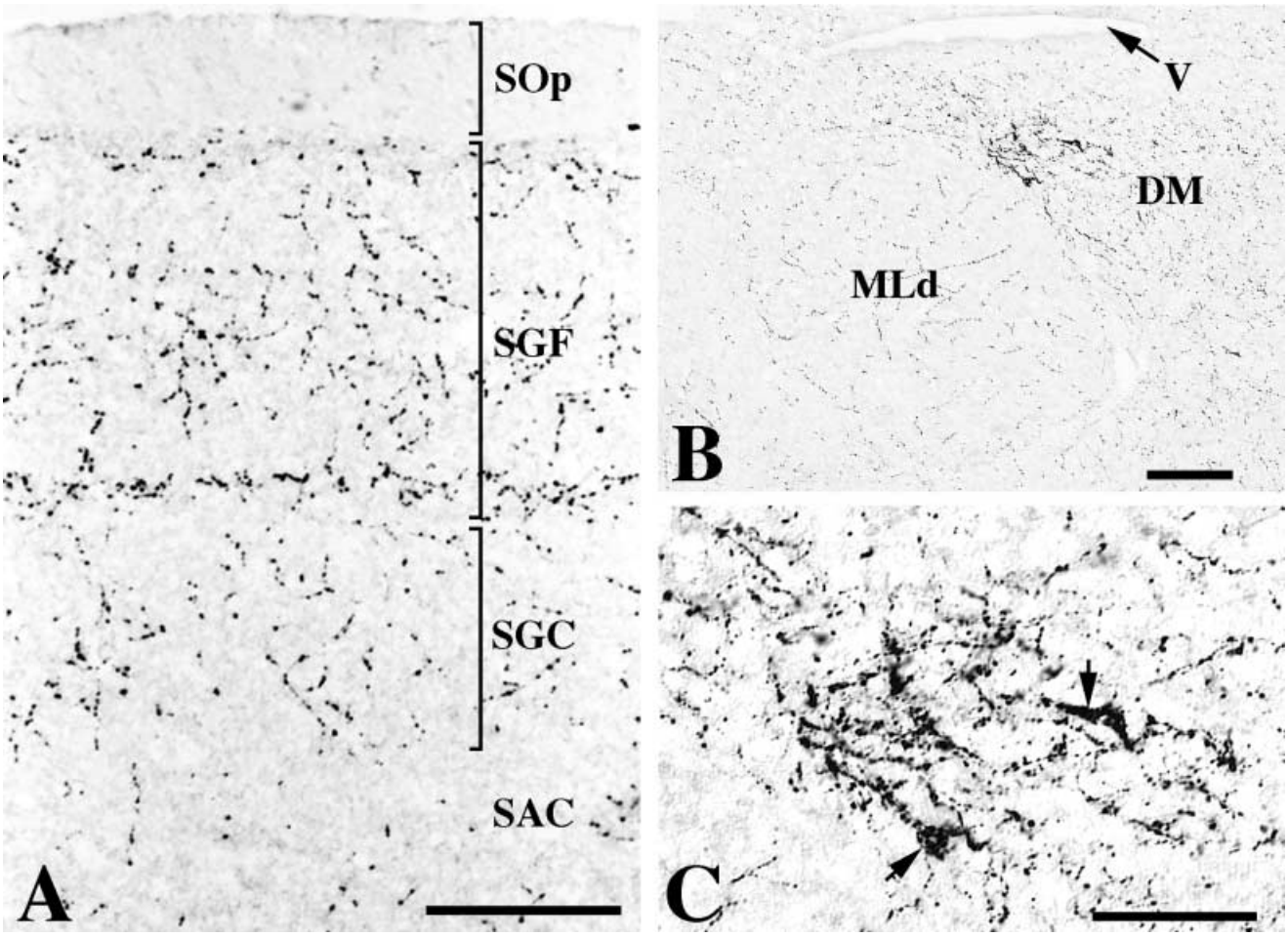

Fig. 13. Photomicrographs depicting DBH-ir elements in the optic tectum and the nucleus intercollicularis (ICo) in a frontal section (same level shown in Fig. 2G). **A:** Note the relatively dense innervation of several layers of the optic tectum, except for the stratum opticum (SOp). **B:** Note the moderate innervation of the auditory nucleus mesencephalicus lateralis, pars dorsalis (MLd), by short labeled processes and granulations; this contrasts with the high density of innervation of the dorsomedial nucleus of the ICo (DM), particularly its most dorsolateral portion. **C:** Detail of DBH staining in DM showing several cell somata and dendritic branches covered with strongly labeled, punctate processes (indicated by arrows). For abbreviations, see list. Scale bars = 100 μm in A,B, 50 μm in C.

staining or were not included in the analysis. Such caveats notwithstanding, the present study, together with the previous descriptions of TH-ir, provides a quite complete picture of the differential distribution of the noradrenergic and dopaminergic systems in the zebra finch brain.

The distribution of DBH-immunopositive cell somata was restricted to the pons and the medulla. Therefore, the previously described TH-positive perikarya in nuclei of the preoptic area and hypothalamus, the surroundings of the pretectal nucleus, the SN, the AVT, the region around the IP, the portion of the GCT dorsolateral to Edinger-Westphal, and the region lateral to the OMv and rostral to the LoC (Bottjer, 1993) most probably correspond to dopaminergic cell somata. One should be aware, however, of the existence of hypothalamic neuronal populations in nonoscines that are TH-positive and DBH-negative but that contain no immunoreactivity for dopamine. Such neuron populations could represent depleted dopaminergic cells or cells that lack the ability to produce dopamine from its immediate precursor, because the enzyme responsible is absent or inactive (for discussions, see Bailhache and Balthazart, 1993; Reiner et al., 1994). In contrast, the DBH-labeled cells in the LoC, SCv, and caudopontine and medullary fields most probably are noradrenergic (however, see discussion above on adrenergic cells). These observations are consistent with the results of the comparative DBH vs. TH analysis performed in both the quail brain and the pigeon brain (Bailhache and Balthazart, 1993; Reiner et al., 1994).

The most marked difference in the distribution of DBH-labeled fibers and terminals, compared with TH-positive fibers and terminals, lies in the almost complete absence of the former from paleostriatal fields. These structures, including song nucleus area X, which is embedded in the LPO, receive dense TH-positive projections from the AVT and the SN (formerly named TPc; Lewis et al., 1981). Because we observed no DBH-stained cell bodies in the AVT or the SN, we conclude that the dense innervation of the paleostriatum by TH-positive elements is most probably dopaminergic in nature. This observation is consistent with the high density of D1 dopamine receptors observed in area X in the surrounding LPO and in the PA of

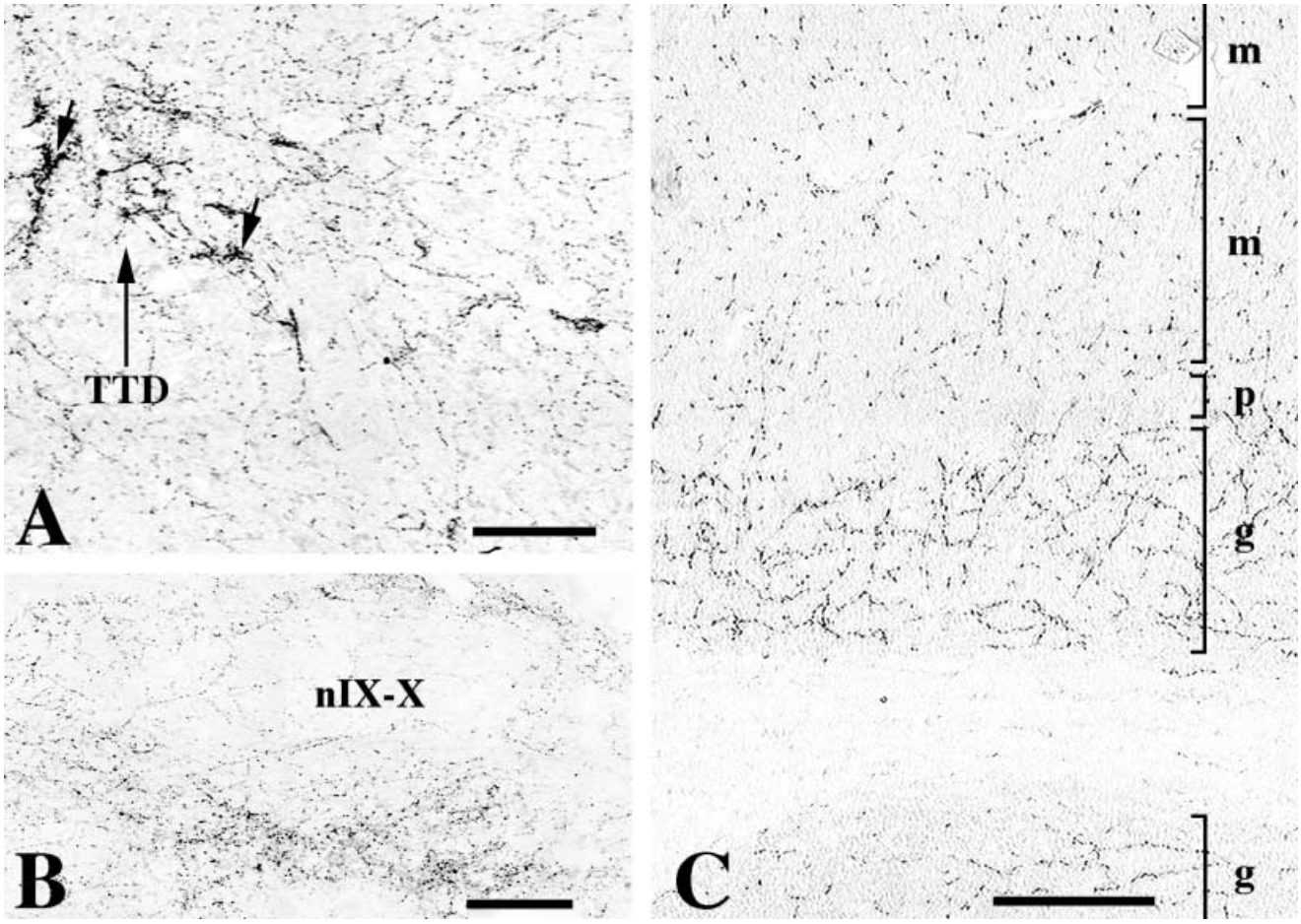

Fig. 14. Photomicrographs depicting DBH-ir elements in the pons, medulla, and cerebellum. **A:** View of the lateral portion of the caudal pons in a frontal section (same level shown in Fig. 2K). Note the presence of various cell somata covered with numerous punctate, DBH-labeled elements (indicated by short arrows). **B:** View of the dorsomedial portion of the medulla at the level of the nucleus of the glossopharyngeal nerve and dorsal motor nucleus of the vagal nerve (nIX–X) in a frontal section (same level shown in Fig. 2M). Note the dense aggregation of DBH-labeled, fine branches and granulations around but not inside nIX–X, particularly ventrally. **C:** View of area in the cerebellar cortex in a parasagittal section (same level shown in Fig. 3B). The highest density of innervation occurs in the granular cell layer (g), whereas the molecular (m) and Purkinje cell (p) layers show lower densities. The molecular layer on top corresponds to the molecular layer in an adjacent fold of the cerebellar cortex. For abbreviations, see list. Scale bars = 100 μm in A,C, 50 μm in B.

songbirds (Casto and Ball, 1994; however, see discussion above on adrenergic receptors). It is also compatible with the view that such a projection represents the avian counterpart of the nigrostriatal dopaminergic projection in mammals (Lewis et al., 1981). Thus, area X could represent a specialization of the avian region that corresponds to the caudate putamen of mammals. It is intriguing to note that area X projects to the DLM, which is a thalamic nucleus (Bottjer et al., 1989), rather than to the PP, the avian globus pallidus (i.e., the mammalian target of the caudate putamen); such a connectivity pattern (striatum to thalamus) is reminiscent of that of the nucleus accumbens (for further discussion, see Bottjer and Johnson, 1997).

A high density of TH-ir elements has also been described in adult finches for other telencephalic song nuclei, including HVC, RA, NIf, and lMAN (Bottjer, 1993; Soha et al., 1996). To various degrees, the density of immunoreactivity was reported to be higher than that of the surrounding tissues for these nuclei. This effect was most conspicuous for HVC and NIf and was less conspicuous for RA and lMAN. By comparison, the density of DBH staining we observed in these areas was only low to moderate and reflected the density of the respective surrounding areas. A major component of the TH-staining pattern within these song nuclei, therefore, appears to consist of dopaminergic fibers and terminals. This conclusion is substantiated further by the biochemical detection and measurement of turn-over rates of dopamine within all of these nuclei (Barclay and Harding, 1988, 1990; Sakaguchi and Saito, 1989; Barclay et al., 1992; Harding et al., 1998); the highest levels were described for area X, which, correspondingly, has the highest density of TH-ir elements (Bottjer, 1993; Soha et al., 1996) and no detectable DBH-ir (present study).

A sex difference in DBH-staining pattern has been detected in the preoptic area of the quail (Bailhache and Balthazart, 1993). Although we did not perform a quantitative analysis, we observed no obvious evidence for sex differences or for developmental modulation of DBH stain-

ing within song nuclei from the age 25 days onward. This suggests that sex or age differences in DBH staining patterns in zebra finches, if they are present, are small, and their demonstration will require careful quantification. The reported sex difference in the density of TH-ir within song control nuclei (Bottjer, 1993), therefore, probably reflects a stronger dopaminergic innervation in males. Similarly, we interpret the reported increase in the density of TH-immunoreactive elements within the HVC and other song control nuclei in juvenile male finches (Soha et al., 1996) as most probably reflecting a gradual increase in the dopaminergic innervation of these nuclei. Compatible with this view, an increase in dopamine content has been observed within the HVC during this period without an apparent increase in norepinephrine levels (Sakaguchi and Saito, 1989).

Although these observations appear to indicate an overall predominance of the dopaminergic innervation in the song system, one should be cautious in their interpretation. Indeed, a more recent study has reported higher levels of both norepinephrine and dopamine in juvenile than in adult zebra finches (Harding et al., 1998). That observation is compatible with a participation of catecholamines in the process of song learning, but is in apparent contrast to the known TH-staining pattern (Bottjer, 1993) and our present DBH-staining results. One should point out, however, as discussed by the authors, that regulation of catalytic activity, rather than content of catecholamine-synthesizing enzymes, may be the critical determinant of catecholamine levels within song nuclei. Therefore, an antinoradrenaline antiserum might be more sensitive to possible sex or developmental differences in the noradrenergic innervation of the song system.

Other than the paleostriatum and the song control system, several other brain areas are also characterized by much higher levels of TH- than DBH-stained fibers and terminals, indicating a predominance of dopaminergic projections over noradrenergic projections. These include the septum, particularly its lateral portion, the ventrolateral hypothalamus, the tuberal region, the pretectal area, the tegmental area, and the substantia nigra. In contrast, there is a relative predominance of DBH in telencephalic regions outside the paleostriatum. Although this partly could reflect a differential sensitivity of the antibodies, the patterns are in general agreement with those reported for other species (Bailhache and Balthazart, 1993; Reiner et al., 1994; Moons et al., 1995) and appear to be a conserved feature of the avian brain. Finally, it is also interesting to note that some areas showing high densities of DBH-ir elements, particularly the pericellular arrays around perikarya and dendrites, contain TH-labeled cell somata, providing a possible site for a strong modulatory influence of noradrenergic cells on the dopaminergic system.

In summary, we have described in detail the noradrenergic system in the brain of zebra finches by using ICC for DBH. For most brain areas, the distribution of DBH-immunoreactive elements is remarkably comparable to that described in nonoscine avian species, indicating a conservation of the general organization of avian noradrenergic projections. A subtractive comparison with previous descriptions of TH-ir allows for a detailed definition of the dopaminergic system in zebra finches. The significant innervation of several auditory processing stations and song control nuclei by DBH-positive fibers lends further support to a participation of noradrenergic mechanisms in the modulation of song perception and production.

ACKNOWLEDGMENTS

The authors thank Daun Jackson, Sharon Sepe, and Helen Ecklund for their attentive bird keeping; Sandy Hills for secretarial aide; Constance Scharff for useful discussions; and Fernando Nottebohm for his continuous support. R.P. thanks Ricardo Gattass, Marcos Palatnik, Claudia Vargas, and Eliane Volchan for their support and encouragement. This work was supported by NIDCD grant DC02853 to C.V.M., by a Kluge fellowship to S.R., and by CNPq and UFRJ fellowships to R.P.

LITERATURE CITED

Arnold, A.P. (1997) Sexual differentiation of the zebra finch song system: Positive evidence, negative evidence, null hypotheses, and a paradigm shift. J. Neurobiol. *33:*572–584.

Bailhache, T. and J. Balthazart (1993) The catecholaminergic system of the quail brain: Immunocytochemical studies of dopamine-β-hydroxylase and tyrosine hydroxylase. J. Comp. Neurol. *329:*230–256.

Ball, G. (1990) Chemical neuroanatomical studies of the steroid-sensitive songbird vocal control system: A comparative approach. In J. Balthazart (ed): Hormones, Brain and Behavior, Vol. 1. Basel: Karger, pp. 148–167.

Ball, G.F. (1994) Neurochemical specializations associated with vocal learning and production in songbirds and budgerigars. Brain Behav. Evol. *44:*234–246.

Ball, G.F., J.M. Casto, and D.J. Bernard (1994) Sex differences in the volume of avian song control nuclei: Comparative studies and the issue of brain nucleus delineation. Psychoneuroendocrinology *19:*485–504.

Balthazart, J., P. Absil, A. Goidart, M. Houbart, N. Harada, and G.F. Ball (1996) Distribution of aromatase-immunoreactive cells in the forebrain of zebra finches (*Taeniopygia guttata*): Implications for the neural action of steroids and nuclear definition in the avian hypothalamus. J. Neurobiol. *31:*129–148.

Barclay, S.R. and C.F. Harding (1988) Androstenedione modulation of monoamine levels and turnover in hypothalamic and vocal control nuclei in the male zebra finch: Steroid effects on brain monoamines. Brain Res. *459:*333–343.

Barclay, S.R. and C.F. Harding (1990) Differential modulation of monoamine levels and turnover rates by estrogen and/or androgen in hypothalamic and vocal control nuclei of male zebra finches. Brain Res. *523:*251–262.

Barclay, S.R., C.F. Harding, and S.A. Waterman (1992) Correlations between catecholamine levels and sexual behavior in male zebra finches. Pharmacol. Biochem. Behav. *41:*195–201.

Bottjer, S.W. (1993) The distribution of tyrosine hydroxylase immunoreactivity in the brains of male and female zebra finches. J. Neurobiol. *24:*51–69.

Bottjer, S.W. and F. Johnson (1997) Circuits, hormones, and learning: Vocal behavior in songbirds. J. Neurobiol. *33:*602–618.

Bottjer, S.W., E.A. Miesner, and A.P. Arnold (1984) Forebrain lesions disrupt development but not maintenance of song in passerine birds. Science *224:*901–903.

Bottjer, S.W., K.A. Halsema, S.A. Brown, and E.A. Miesner (1989) Axonal connections of a forebrain nucleus involved with vocal learning in zebra finches. J. Comp. Neurol. *279:*312–326.

Casto, J.M. and G.F. Ball (1994) Characterization and localization of D1 dopamine receptors in the sexually dimorphic vocal control nucleus, area X, and the basal ganglia of European starlings. J. Neurobiol. *25:*767–780.

Casto, J.M. and G.F. Ball (1996) Early administration of 17β-estradiol partially masculinizes song control regions and a_2-adrenergic receptor distribution in European Starlings (*Sturnus vulgaris*). Hormone Behav. *30:*387–406.

Chew, S.J., C.V. Mello, F. Nottebohm, E. Jarvis, and D. Vicario (1995) Decrements in auditory responses to a repeated conspecific song are long-lasting and require two periods of protein synthesis in the songbird forebrain. Proc. Natl. Acad. Sci. USA *92:*3406–3410.

Cirelli, C., M. Pompeiano, and G. Tononi (1996) Neuronal gene expression in the waking state: A new role for the locus coeruleus. Science *274:*1211–1215.

Durand, S.E., J.M. Tepper, and M.-F. Cheng (1992) The shell region of the nucleus ovoidalis: A subdivision of the avian auditory thalamus. J. Comp. Neurol. *323:*495–518.

Eales, L.A. (1985) Song learning in zebra finches: Some effects of song model availability on what is learnt and when. Anim. Behav. *33:*1293–1300.

Eales, L.A. (1987) Song learning in female-raised zebra finches: Another look at the sensitive phase. Anim. Behav. *35:*1356–1365.

Everitt. B.J., T.W. Robbins, M. Gaskin, and P.J. Fray (1983) The effects of lesions to ascending noradrenergic neurons on discrimination learning and performance in the rat. Neuroscience *10:*397–410.

Fortune, E.S. and D. Margoliash (1992) Cytoarchitectonic organization and morphology of cells of the Field L complex in male zebra finches (*Taeniopygia guttata*). J. Comp. Neurol. *325:*388–404.

Fortune, E.S. and D. Margoliash (1995) Parallel pathways and convergence onto HVc and adjacent neostriatum of adult zebra finches (*Taeniopygia guttata*). J. Comp. Neurol. *360:*413–441.

Harding, C.F., S.R. Barclay, and S.A. Waterman (1998) Changes in catecholamine levels and turnover rates in hypothalamic, vocal control, and auditory nuclei in male zebra finches during development. J. Neurobiol. *34:*329–346.

Hökfelt, T., R. Martensson, A. Björklund, S. Kleinau, and M. Goldstein (1984) Distributional maps of tyrosine hydroxylase-immunoreactive neurons in the rat brain. In A. Björklund and T. Hökfelt (eds): Handbook of Chemical Neuroanatomy, Vol. 2, Classical Transmitters in the CNS, Part I. Amsterdam: Elsevier, pp. 277–379.

Hopkins, W.F. and D. Johnston (1984) Frequency-dependent noradrenergic modulation of long-term potentiation in the hippocampus. Science *226:*350–352.

Immelman, K. (1969) Song development in the zebra finch and other estrildid finches. In R.A. Hinde (ed): Bird Vocalizations. Cambridge: Cambridge University Press, pp. 61–77.

Jarvis, E. and F. Nottebohm (1997) Motor-driven gene expression. Proc. Natl. Acad. Sci. USA *94:*4097–4102.

Johnson, F., M.M. Sablan, and S.W. Bottjer (1995) Topographic organization of a forebrain pathway involved with vocal learning in zebra finches. J. Comp. Neurol. *358:*260–278.

Karter, J.H. and W. Hodos (1967) A Stereotoxic Atlas of the Brain of the Pigeon (Columba livia) Baltimore, MD: Johns Hopkins Press.

Kelley, D.B. and F. Nottebohm (1979) Projections of a telencephalic auditory nucleus—field L—in the canary. J. Comp. Neurol. *183:*455–470.

Konishi, M. (1965) The role of auditory feedback in the control of vocalization in the white-crowned sparrow. Z. Tierpsychol. *22:*770–783.

Kroodsma, D.E. (1982) Learning and the ontogeny of sound signals in birds. In D.E. Kroodsma, E.H. Miller, and H. Ouellet (eds): Acoustic Communication in Birds. New York: Academic Press, pp. 1–23.

Kuenzel, W.J. and M. Masson (1988) A Stereotaxic Atlas of the Brain of the Chick (*Gallus domesticus*). Baltimore: Johns Hopkins University Press.

Lewis, J.W., S.M. Ryan, A.P. Arnold, and L.L. Butcher (1981) Evidence for a catecholaminergic projection to area X in the zebra finch. J. Comp. Neurol. *196:*347–354.

Marler, P. and S. Peters (1977) Selective vocal learning in a sparrow. Science *198:*519–527.

Marler, P. and S. Peters (1981) Sparrows learn adult song and more from memory. Science *213:*780–782.

Marler, P. and S. Peters (1982) Long-term storage of learned bird songs prior to production. Anim. Behav. *30:*479–482.

Marler, P. and M. Tamura (1964) Culturally transmitted patterns of vocal behavior in sparrows. Science *146:*1483–1486.

McGaugh, J.L. (1989) Involvement of hormonal and neuro-modulatory systems in the regulation of memory storage. Annu. Rev. Neurosci. *12:*255–287.

Mello, C.V. and D.F. Clayton (1994) Song-induced ZENK gene expression in auditory pathways of songbird brain and its relation to the song control system. J. Neurosci. *14:*6652–6666.

Mello, C.V. and S. Ribeiro (1998) ZENK protein regulation by song in the brain of songbirds. J. Comp. Neurol. *393:*426–438.

Mello, C.V., G.E. Vates, S. Okuhata, and F. Nottebohm (1998) Descending auditory pathways in the adult male zebra finch (*Taeniopygia guttata*). J. Comp. Neurol. *395:*137–160.

Moons, L., E. D'Hondt, K. Pijcke, and F. Vandesande (1995) Noradrenergic system in the chicken brain: Immunocytochemical study with antibodies to noradrenaline and dopamine-β-hydroxylase. J. Comp. Neurol. *360:*331–348.

Nottebohm, F. (1968) Auditory experience and song development in the chaffinch, *Fringilla coelebs*. Ibis *110:*549–568.

Nottebohm, F. (1972) The origins of vocal learning. Am. Nature *106:*116–140.

Nottebohm, F., T.M. Stokes, and C.M. Leonard (1976) Central control of song in the canary, *Serinus canaria*. J. Comp. Neurol. *165:*457–486.

Nottebohm, F., D.B. Kelley, and J.A. Paton (1982) Connections of vocal control nuclei in the canary telencephalon. J. Comp. Neurol. *207:*344–357.

Okuhata, S. and N. Saito (1987) Synaptic connections of thalamo-cerebral vocal nuclei of the canary. Brain Res. Bull. *18:*35–44.

Reiner, A., E.J. Karle, K.D. Anderson, and L. Medina (1994) Catecholaminergic perikarya and fibers in the avian nervous system. In W.J.A.J. Smeets and A. Reiner (eds): Phylogeny and Development of Catecholamine Systems in the CNS of Vertebrates. Cambridge: Cambridge University Press, pp. 135–181.

Sakaguchi, H and N. Saito (1989) The acetylcholine and catecholamine contents in song control nuclei of zebra finch during song ontogeny. Dev. Brain Res. *47:*313–317.

Scharff, C. and F. Nottebohm (1991) A comparative study of the behavioral deficits following lesions of various parts of the zebra finch song system: Implications for vocal learning. J. Neurosci. *11:*2896–2913.

Soha, J.A., T. Shimizu, and A.J. Doupe (1996) Development of the catecholaminergic innervation of the song system of the male zebra finch. J. Neurobiol. *29:*473–489.

Sohrabji, F., E.J. Nordeen, and K.W. Nordeen (1990) Selective impairment of song learning following lesions of a forebrain nucleus in the juvenile zebra finch. Behav. Neural Biol. *53:*51–63.

Steeves, J.D., C.A. Taccogna, K.A. Bell, and S.R. Vincent (1987) Distribution of phenylethanolamine-N-methyltransferase (PNMT)-immunoreactivity neurons in the avian brain. Neurosci. Lett. *76:*7–12.

Stokes, T.M., C.M. Leonard, and F. Nottebohm (1974) The telencephalon, diencephalon, and mesencephalon of the canary, *Serinus canaria*, in stereotaxic coordinates. J. Comp. Neurol. *156:*317–374.

Sullivan, R.M., D.A. Wilson, and M. Leon (1989) Norepinephrine and learning-induced plasticity in infant rat olfactory system. J. Neurosci. *9:*3998–4006.

Thorpe, W.H. (1958) The learning of song patterns by birds, with special reference to the song of the chaffinch, *Fringilla coelebs*. Ibis *100:*535–570.

Tillet, Y. (1988) Adrenergic neurons in sheep brain demonstrated by immunohistochemistry with antibodies to phenylethanolamine *N*-methyltransferase (PNMT) and dopamine-β-hydroxylase (DBH): Absence of the C cell group in the sheep brain. Neurosci. Lett. *95:*107–112.

Vates, G.E. and F. Nottebohm (1995) Feedback circuitry within a song learning pathway. Proc. Natl. Acad. Sci. USA *92:*5139–5143.

Vates, G.E., B.M. Broome, C.V. Mello, and F. Nottebohm (1996) Auditory pathways of caudal telencephalon and their relation to the song system of adult male zebra finches (*Taenopygia guttata*). J. Comp. Neurol. *366:*613–642.

Vicario, D.S. (1991) Organization of the zebra finch song control system: II. Functional organization of outputs from nucleus robustus archistriatalis. J. Comp. Neurol. *309:*486–494.

Vicario, D.S. (1993) A new brainstem pathway for vocal control in the zebra finch song system. Neuroreport *4:*983–986.

Vicario, D.S. and F. Nottebohm (1990) Organization of the zebra finch song control system: I. Representation of syringeal muscles in the hypoglossal nucleus. J. Comp. Neurol. *271:*346–354.

Wild, J.M. (1993) Descending projection of the songbird nucleus robustus archistriatalis. J. Comp. Neurol. *338:*225–241.

Wild, J.M. (1994) The auditory-vocal-respiratory axis in birds. Brain Behav. Evol. *44:*192–209.

Wild, J.M. (1997) Neural pathways for the control of birdsong production. J. Neurobiol. *33:*653–670.

Wild, J.M., H.J. Karten, and B.J. Frost (1993) Connections of the auditory forebrain in the pigeon (*Columba livia*). J. Comp. Neurol. *337:*32–62.

Wilson, D.A., T-C. Pham, and R.M. Sullivan (1994) Norepinephrine and posttraining memory consolidation in neonatal rats. Behav. Neurosci. *108:*1053–1058.

Yu, A.C. and D. Margoliash (1996) Temporal hierarchical control of singing in birds. Science *273:*1871–1875.